Composite waste wax as phase change material for energy storage using in portable device

Naruemon Nakmueng
Aroonroj Chaosukho

A Report Submitted in Partial Fulfillment of the Requirements
for the Degree of Bachelor of Engineering (Petrochemical Engineering)
Department of Chemical Engineering, Faculty of Engineering,
King Mongkut's Institute of Technology Ladkrabang
Academic Year 2019

สารเปลี่ยนวัฏภาคจากไขเหลือทิ้งอุตสาหกรรม
สำหรับการกักเก็บพลังงานที่ใช้ในอุปกรณ์พกพา

นฤมล นาคเมือง

อรุณโรจน์ เชาว์สุโข

ปริญญานิพนธ์นี้เป็นส่วนหนึ่งของการศึกษาตามหลักสูตร

วิศวกรรมศาสตรบัณฑิต สาขาวิชาวิศวกรรมปิโตรเคมี

ภาควิชาวิศวกรรมเคมี คณะวิศวกรรมศาสตร์

สถาบันเทคโนโลยีพระจอมเกล้าเจ้าคุณทหารลาดกระบัง

ปีการศึกษา 2562

Title	Composite waste wax as phase change material for energy storage using in portable device
By	Miss Naruemon Nakmueng and Miss Aroonroj Chaosukho
Field of Study	Petrochemical Engineering
Advisor	Asst.Prof.Dr. Tanawan Pinnarat

Accepted by the Faculty of Engineering, King Mongkut's Institute of Technology Ladkrabang in Partial Fulfillment of the Requirements for the Degree of Bachelor of Engineering (Petrochemical Engineering).

Thesis Committee

Tanawan Pinnarat. _____ Chairman

(Asst.Prof.Dr. Tanawan Pinnarat)

Natthanon Phaiboonsilpa _____ Committee

(Asst.Prof.Dr. Natthanon Phaiboonsilpa)

T. Samanmulya _____ Committee

(Asst.Prof.Dr. Thachanan Samanmulya)

Title	Composite waste wax as phase change material for energy storage using in portable device
By	Miss Naruemon Nakmueng and Miss Aroonroj Chaosukho
Advisor	Asst.Prof.Dr. Tanawan Pinnarat
Field of Study	Petrochemical Engineering
Affiliation	Department of Chemical Engineering, Faculty of Engineering, King Mongkut's Institute of Technology Ladkrabang

Abstract

The waste waxes are mixed with an additive to produce composite phase change material (CPCM) to apply to thermal energy storage (TES) application. Differential scanning calorimeter (DSC) results showed that palm wax has higher latent heat, less volume change and does not have superheating and subcooling phenomena compared to rice bran wax. Therefore, palm wax was chosen to make composite material. Reduced graphene oxide (rGO) and activated carbon (AC) used to enhance thermal conductivity (k) of PCM. From SEM analysis, AC has similar structure with graphite, so AC has good conductivity and less expensive compared to rGO. Therefore, AC was used as an additive for CPCM. AC are varied from 0.0 wt%, 0.5 wt%,1.0 wt%, 1.5 wt%, 2.0 wt%, and 2.5 wt% in CPCM. TCA analysis showed 14.42% increase of thermal conductivity for 2.5 wt% AC when compared with pure palm wax (k of pure palm wax = 0.208 ± 0.001 W/m·K, k of 2.5 wt% of AC in CPCM = 0.238 ± 0.002 W/m·K). The thermal conductivity increases with increasing amount of AC. However, latent heat (ΔH) was decreased by 15.92% when compared to pure palm wax (ΔH of pure palm wax = 197.31 ± 15.970 J/g, ΔH of 2.5 wt% of AC in CPCM = 165.90 $\pm$ 9.810 J/g). Prototype of portable device with 2.5 wt% AC CPCM enhanced the charging time (t) by 45.9% when compared with portable device without CPCM (t of device without CPCM = 93 ± 3.464 minutes, t of device with CPCM = 172 ± 5.540 minutes). Moreover, the power (Q) from calculation of device without CPCM and with CPCM are 80.9 kW and 81.4 kW respectively. The results concluded that CPCM can be used to enhance thermal properties by adding high thermal conductivity material (AC) and can be used to produce electricity from applying with TES application.

Keywords: Phase change material, Thermal energy storage, Palm wax, Portable device

เรื่อง สารเปลี่ยนวัฏภาคจากไขเหลือทิ้งอุตสาหกรรมสำหรับการกักเก็บพลังงานที่ใช้ในอุปกรณ์พกพา

โดย นางสาวนฤมล นาคเมือง และนางสาวอรุณโรจน์ เชาว์สุโข

อาจารย์ที่ปรึกษา ผศ.ดร.ธนวรรณ พิณรัตน์

สาขาวิชา วิศวกรรมวิชาปิโตรเคมี

สังกัด ภาควิชาวิศวกรรมเคมี คณะวิศวกรรมศาสตร์
สถาบันเทคโนโลยีพระจอมเกล้าเจ้าคุณทหารลาดกระบัง

บทคัดย่อ

ไขเหลือทิ้งถูกนำมาผสมกับสารเติมแต่งเพื่อผลิตสารเปลี่ยนวัฏภาคแบบคอมโพสิต สำหรับการนำประยุกต์ใช้กับการเก็บพลังงานความร้อน ผลจากการวิเคราะห์โดยใช้เครื่องวัดค่าความต่างความร้อนของสาร (DSC) พบว่าไขปาล์มมีค่าความร้อนแฝงที่สูง การเปลี่ยนแปลงของปริมาตรน้อย และไม่เกิดสภาวะร้อนยวดยิ่งและสภาวะเย็นยิ่งยวดเมื่อเปรียบเทียบกับไขข้าว ไขปาล์มจึงถูกนำมาใช้เพื่อผลิตสารเปลี่ยนวัฏภาคแบบคอมโพสิต รีดิวซ์แกรฟีนออกไซด์และถ่านกัมมันต์ถูกนำมาใช้เพื่อศึกษาเป็นสารเติมแต่งที่ใช้สำหรับเพิ่มค่าการนำความร้อนของสารเปลี่ยนวัฏภาค การวิเคราะห์โดย SEM แสดงให้เห็นว่าถ่านกัมมันต์มีโครงสร้างที่คล้ายกับกราไฟต์ซึ่งมีค่าการนำไฟฟ้าที่ดี และมีราคาถูกเมื่อเปรียบเทียบกับรีดิวซ์แกรฟีนออกไซด์ ถ่านกัมมันต์จึงถูกนำมาใช้เป็นสารเติมแต่งในการผลิตสารเปลี่ยนวัฏภาคแบบคอมโพสิต ซึ่งสารเปลี่ยนวัฏภาคแบบคอมโพสิตถูกนำมาเตรียมในอัตราร้อยละโดยมวลคือ 0.0, 0.5, 1.0, 1.5, 2.0 และ 2.5 ของถ่านกัมมันต์ การวิเคราะห์โดย TCA แสดงให้เห็นถึงการนำความร้อนเพิ่มขึ้น 14.42% ที่ความเข้มข้น 2.5 ร้อยละโดยมวลของถ่านกัมมันต์เมื่อเปรียบเทียบกับไขปาล์ม (ค่าการนำความร้อนของไขปาล์มเท่ากับ 0.208 ± 0.001 วัตต์ต่อเมตร-เคลวิน, ที่ความเข้มข้น 2.5 ร้อยละโดยมวลของถ่านกัมมันต์ในสารเปลี่ยนวัฏภาคแบบคอมโพสิตเท่ากับ 0.238 ± 0.002 วัตต์ต่อเมตร-เคลวิน) ซึ่งการนำความร้อนจะเพิ่มขึ้นตามปริมาณของถ่านกัมมันต์ที่เพิ่มขึ้น อย่างไรก็ตามค่าความร้อนแฝงที่ความเข้มข้น 2.5 ร้อยละโดยมวลของถ่านกัมมันต์โดยมีค่าลดลง 15.92% ของค่าความร้อนแฝงเมื่อเปรียบเทียบกับไขปาล์ม (ความร้อนแฝงของไขปาล์มเท่ากับ 197.31 ± 15.970 จูลต่อกรัม, ความร้อนแฝงที่ความเข้มข้น 2.5 ร้อยละโดยมวลของถ่านกัมมันต์ในสารเปลี่ยนวัฏภาคแบบคอมโพสิตเท่ากับ 165.90 ± 9.810 จูลต่อกรัม) นอกจากนี้อุปกรณ์แบบพกพาที่บรรจุสารเปลี่ยนวัฏภาคแบบคอมโพสิตที่ความเข้มข้น 2.5 ร้อยละโดยมวลของถ่านกัมมันต์มีประสิทธิภาพดีขึ้น 45.9% เมื่อเปรียบเทียบกับอุปกรณ์พกพาที่ไม่มีการบรรจุสารเปลี่ยนวัฏภาคแบบคอมโพสิต (เวลาของอุปกรณ์พกพาที่ไม่มีสารเปลี่ยนวัฏภาคแบบคอมโพสิตหยุดปล่อยกระแสไฟเท่ากับ 93 ± 3.464 นาที, เวลาของอุปกรณ์พกพาที่มีสารเปลี่ยนวัฏภาคแบบคอมโพสิตหยุดปล่อยกระแสไฟเท่ากับ 172 ± 5.540นาที)

นอกจากนี้กำลังไฟฟ้าจากการคำนวณอุปกรณ์ที่ไม่มีสารเปลี่ยนวัฏภาคแบบคอมโพสิต และมีสารเปลี่ยนวัฏภาคแบบคอมโพสิต คือ 80.9 กิโลวัตต์ และ 81.4 กิโลวัตต์ ตามลำดับผลสรุปได้ว่าสารเปลี่ยนวัฏภาคแบบคอมโพสิตสามารถปรับปรุงคุณสมบัติทางความร้อนโดยการเติมวัสดุที่มีค่าการนำความร้อนสูงและสามารถใช้ในการผลิตกระแสไฟฟ้าโดยการประยุกต์กับการกักเก็บความร้อนได้

คำสำคัญ: สารเปลี่ยนวัฏภาค, การกักเก็บความร้อน, ไขปาล์ม, อุปกรณ์พกพา

Acknowledgements

I would like to express my sincere thanks to my advisor Asst.Prof. Dr Tanawan Pinnarat who provides me the opportunity to undertake the excellent project on the topic composite waste wax as phase change material for energy storage using in portable device. My advisor also supports me in the research, provides scholarship for the purchase of project equipment and suggests guidelines for completing this project.

I am grateful for the committee member, Asst.Prof.Dr. Natthanon Phaiboonsilpa and Asst.Prof.Dr. Thachanan Samanmulya, for their suggestion and assistance on appropriate research development.

I would also like to thank Department of Chemical Engineering, King Mongkut's Institute of Technology Ladkrabang and department engineer, Mr. Pisan Ponpo, for suggesting good technique of the equipment usage and supporting workspace.

Finally, I most gratefully all professors in the department for providing the knowledges and experiences in the bachelor’s degree which are important for research development.

Naruemon Nakmueng and Aroonroj Chaosukho

Table of Contents

Table of Contents (Cont.)

List of Figures

List of Figures (Cont.)

Page

List of Tables

List of Tables (Cont.)

Page

NOMENCLATURE

A_i	Area of surface, m^2
A_s	Heat transfer surface area, m^2
$F_{i \rightarrow j}$	View factor
g	Gravitational acceleration, m/s^2
H	Height from the base, m
h	Heat transfer coefficient, $W/m^2 \cdot K$
J	Radiosities
k	Thermal conductivity of material, W/m•K
L	Thickness of the medium, m
L_c	Distance between the hot and cold surfaces, m
L_v	High vertical, m
N	Number of surfaces of the enclosure
Nu	Nusselt number
Pr	Prandtl number
Q	Power, W
Q_{CPCM}	Latent heat of composite phase change material, W
$Q_{conduction}$	Heat of conduction, W
$Q_{convection}$	Heat of convection, W
$Q_{radiation}$	Heat of radiation, W
R	Thermal resistance, ºC/W
Ra_L	Rayleigh number for enclosure
R_{total}	Total thermal resistance, ºC/W
T_f	Film temperature, ºC
T_i	Temperature, ºC
T_s	Temperature of the surface, ºC
T_1	Temperature of hot surfaces, ºC
T_2	Temperature of cold surfaces, ºC
T_∞	Temperature of the fluid sufficiently far from the surface, ºC
W	Wide of the medium, m
σ	Stefan-boltzmann constant, $W/m^2 K^4$
ε_i	Emissivity of the surface
β	Coefficient of volume expansion, 1/K ($\beta = 1/T_f$ for ideal gases)

v	Kinematic viscosity of the fluid, m^2/s

Subscripts

AC	Activated carbon
ANG	Adsorbed Natural Gas
BET	Brunauer-Emmett-Teller
CPCM	Composite phase change material
CPCMs	Composite phase change materials
CSAC	Coconut shell activated carbon
CW	Carnauba wax
DC	Direct current
DICO	Diffusivity and conductivity
DSC	Differential Scanning Calorimeter
EG	Expanded graphite
ENG	Expanded natural graphite
FTIR	Fourier Transform Infrared spectrometer
GO	Graphene oxide
GR	Graphene
HGNF	Herringbone style graphite nanofibers
HRTEM	High-resolution transmission electron microscopy
KOH	Potassium hydroxide
MWCNTs	Multiwalled carbon nanotubes
NePCMs	Nano-enhanced phase change materials
PACC	Paraffin activated carbon composite
PCM	Phase change material
PCMs	Phase change materialห
PCNC	Paraffin multiwalled carbon nanotube composite
PS	Polystyrene
rGO	Reduced graphene oxide
RPM	Revolution per min
SEER	Seasonal Energy Efficiency Ratio
SEM	Scanning Electron Microscopy
SSL	Sodium stearoyl lactylate

TEG	Thermoelectric generator
TEM	Transmission electron microscopy
TES	Thermal energy storage
TGA	Thermogravimetric analysis
THB-method	Transient Hot-Bridge method
TPS	Transient plane source
XPS	X-ray photoelectron spectroscope
XRD	X-ray diffraction

CHAPTER I
INTRODUCTION

1.1 Background

Clean energy is a safe alternative environmentally friendly energy obtained from natural processes such as solar, wind, geothermal, hydropower, ocean, and biomass. The development of clean energy is necessary to reduce global warming and reduce amount of petroleum-based energy consumption. The clean energy is used in transportation, heating and cooling, as well as electricity sectors.

Electrical energy can be derived from energy harvesting technology that converts ambient energy for amassment in devices to electrical energy [1]. Sources of energy harvesting are classified into two groups consist of artificial sources and natural sources. The natural sources are more popular than artificial sources due to extra energy cost reduction [2], for examples, photovoltaic panels, water turbines, electric wind turbines and phase change materials. These energies can be obtained from solar, water, wind, and biomass (including industrial residues).

Thermal energy storage (TES) technology is applied to store the thermal energy, which including sensible heat, latent heat, and chemical energy. Large amount of thermal energy can be stored and released during phase transition of the substances. These substances are called phase change materials (PCMs).

Phase change materials have the potential of providing a more efficient means of storage. Source of phase change materials consists of inorganic and organic materials. For inorganic, the advantages are sharp transitions at the melting point, high thermal conductivity, and high phase change enthalpy but exhibit disadvantages with corrosion, irritant, subcooling, phase segregation and lack of thermal stability. On the other hand, the advantages of organic phase change materials include high specific heat, chemical and thermal stability, relatively high heat of fusion and non-corrosives. Disadvantages include low thermal conductivity, Instability at high temperatures and flammability.

However, high conductivity materials were studied to improve properties of organic phase change materials. Many reports offered various additive materials to increase the thermal conductivity of PCMs such as metal particles [3, 4], metal foam [5, 6], expanded graphite [7] and carbon nanotubes [8, 9].

Material usually use for organic phase change material is natural wax, which are used in many applications such as the production of coatings, used as ingredients in the cosmetics, food, and pharmaceutical industries. Natural waxes are classified into vegetable wax and animal wax. The former is preferred for PCM, example of vegetable wax PCM is carnauba wax. Carnauba wax has suitable properties for PCM. However, it is quite expensive. Therefore, it would be attractive if waste wax from the production process can be used. In this study, palm wax and rice bran wax, which are by-product from the process, were investigated to find the potential as PCMs material. In addition, activated carbon and reduced graphene oxide ware chosen as an additive for thermal conductivity improvement.

1.2 Objectives

1.2.1 To study the possibility of using waste wax from the production process as a phase change material (PCM) in heat storage process.

1.2.2 To study the improvement of electrical conductivity of PCM by mixing activated carbon and reduced graphene oxide.

1.2.3 To design and make a prototype of a portable device producing electricity from thermal energy transformation using phase change material to prolong the process.

1.3 Scopes of work

1.3.1 Waste waxes, which are used in the studied, are palm wax and rice bran wax.

1.3.2 Improve thermal and electrical conductivities of waste waxes by adding rGO in the amount at 0.5 wt%, 1.0 wt% and activated carbon in amount of 0.5 wt%, 1.0 wt%, 1.5 wt%, 2.0 wt%, and 2.5 wt% respectively.

1.3.3 Prototype of portable device with cost efficiency.

1.4 Expect outputs

1.4.1 The idea can be applied for the industrial scale by using heat storage obtained from production process waste and can be commercially available for portable devices.

1.4.2 The heat storage device can be used as a learning equipment in Chemical Engineering Thermodynamics and Heat Transfer classes.

CHAPTER II
LITERATURE REVIEW

Phase Change Materials (PCMs) are latent heat storage materials that can store large amounts of energy with almost no loss and discharge them again later. When the source of temperature increases, the chemical bonding within the PCM breaks up due to the material changes phase from solid to liquid such as in the case for solid-liquid PCM. In a heat storage process occurs in the storage material, the material starts to melt as the phase change temperature is reached. The temperature stays nearly constant until the melting process is finished. The heat is stored during the phase change process (melting process) of the material is called the latent heat. Latent heat storage can be used in a wide range of temperatures. Many PCMs are known to melt with a heat of fusion in any required range [10].

2.1 Suitable properties of PCM for thermal storage application

The PCM that will be used for thermal storage system should have the desired thermo-physical, kinetic, and chemical properties.

- **Thermo-physical properties of PCM**

  - The melting temperature is within the desired operating temperature range.

  - The latent heat of fusion per unit volume is high. Thus, the required volume of the container to store a given amount of energy is less.

  - The specific heat is high to provide for additional significant sensible heat storage.

  - The thermal conductivity of both solid and liquid phases is high to assist in charge and discharge energy of the storage systems.

  - Small volume changes on phase transformation and small vapor pressure at operating temperatures to decrease the containment problem.

- **Kinetic Properties of PCM**

  - The nucleation rate is high to avoid the supercooling of the liquid phase.

  - The rate of crystal growth is high. Therefore, the system can meet demands of heat recovery from the storage system.

- **Chemical properties of PCM**
  - Chemical stability.
  - Complete reversible freeze/melt cycle.
  - No degradation after large number of solidified / melt cycles.
  - Non-corrosiveness to the construction materials.
  - Non-toxic, non-flammable, and non-explosive materials for safety.

2.2 Classification of PCM

PCM can be classified into four different types including solid-solid, solid-liquid, solid-gas and liquid-gas. Of these four types, the solid-liquid PCM are the most suitable for storing thermal energy, where the solid-liquid PCM can be found as organic PCM, inorganic PCM, and eutectics. In addition, organic phase change material is divided into paraffin and non-paraffin compound, inorganic phase change material is divided into salt hydrate and metallic and eutectic phase change material is also divided into organic-organic, inorganic-inorganic, and inorganic-organic [11]. The advantages and disadvantages of each types are summarized in table 1.

Table 1 Advantages and disadvantages of phase change material (Solid-liquid)

PCM			Property	Advantage	Disadvantage	Example	Reference
Organic PCM	Non-paraffin	Fatty acid	$CH_3(CH_2)_{2n}COOH$	- Suitable phase change temperature - High heat of fusion - Easily producible from common vegetable and animal oils - Thermally stable (after repeated melting/freezing cycles) - Less supercooling	- Low thermal conductivity - Flammability - Varying levels of toxicity - Instability at high temperature	- Capric acid (55 wt%) + Expanded perlite (45 wt%) - Lauric acid ($C_{11}H_{23}COOH$) - Myristic acid ($C_{13}H_{27}COOH$) - Palmitic acid ($C_{15}H_{31}COOH$) - Palmitic acid (80 wt%) + Expanded graphite (20 wt%) - Palmitic acid-TiO_2 composite - Stearic acid ($C_{17}H_{35}COOH$) - Sebacic acid ($HOOC(CH_2)_8COOH$)	[12,13]
		Other non-paraffin organic (i.e., esters, alcohol, glycols, etc.)		- Suitable phase change temperature - High heat of fusion - Easily producible from common vegetable and animal oils	- Low thermal conductivity - Flammability - Varying levels of toxicity - Instability at high temperature	- Acetamide (CH_3CONH_2) - Acetanilide (C_8H_9NO) - Benzamide - Erythritol - Methyl palmitate - Methyl stearate - Urea - D-mannitol 99% - Myo-inositol 98% - Galactitol 97%	[12,13]

Table 1 Advantages and disadvantages of phase change material (Solid-liquid) (Cont.)

PCM		Property	Advantage	Disadvantage	Example	Reference
Organic PCM	Paraffins	- C_nH_{2n+2} - Melting temperature range from 23 °C to 67 °C - Volume increases upon melting is in the order of 10 vol.% - Insoluble in water	- Wide range of the phase change temperature - High heat of fusion - Less supercooling - Stable behavior - Less expensive - Ecologically harmless - Non-toxic	- Low thermal conductivity - Moderate flammability	- Paraffin (70 wt%) + Polypropylene (30 wt%) - Paraffin ($C_{22.2}H_{44.1}$) (technical grade) - Paraffin ($C_{23.2}H_{48.4}$) (technical grade) - Paraffin wax 53 (commercial grade) - n-heptadecane/Poly methyl methacrylate ($C_{17}H_{36}$) - n-eicosane (C_{20})	[12,14]
Inorganic PCM	Salt hydrate	- Salt hydrates are alloys of members of the inorganic salt family (oxides, carbonates, sulfates, and nitrates) with water molecules with a specific ratio.	- High thermal conductivity - Sharp transitions at the melting point - High latent heat - Higher densities than organic - Low cost	- Chemical instability - Lose some water content after every heating cycle - High degree of supercooling - Can be corrosive to metals - Lack of thermal stability - Super-cooling	- Calcium chloride hexahydrate ($CaCl_2 \cdot 6H_2O$) - Magnesium chloride hexahydrate ($MgCl_2 \cdot 6H_2O$) - Sodium acetate trihydrate ($NaCH_3COO \cdot 3H_2O$) - $Na_2SO_4 \cdot nH_2O$	[12,15]

Table 1 Advantages and disadvantages of phase change material (Solid-liquid) (Cont.)

PCM		Property	Advantage	Disadvantage	Example	Reference
Inorganic PCM	Metallic	- This group consists of the low melting metals and metal alloys.	- High heat of fusion per unit volume - Higher thermal conductivity - High physical and chemical stability	- Weight issues		[12]

2.3 Heat transfer equation

Heat transfer is classified into plenty of mechanisms including heat of radiation, heat of convection, heat of conduction, and transfer of energy by phase changes.

2.3.1 Heat of radiation

The summation rule is used to a calculator in order to obtain the view factor of each surface in enclosure system which can be expressed as

$$\sum_{i=1}^{N} F_{i\rightarrow j} = 1 \quad (1)$$

Where N is number of surfaces of the enclosure

$F_{i\rightarrow j}$ is view factor

The view factor of each surface can be used to determine the radiosities by equation of surfaces with specified temperature which can be expressed as

$$\sigma T_i^4 = J_i + \frac{1-\varepsilon_i}{\varepsilon_i} \sum_{i=1}^{N} F_{i\rightarrow j} (J_i - J_j) \quad (2)$$

Where J is radiosities

σ is Stefan-boltzmann constant, $W/m^2 \cdot K^4$

T_i is temperature, ^oC

ε_i is emissivity of the surface

N is number of surfaces of the enclosure

The net rates of radiation heat transfer at surfaces are determined from equation

$$Q = A_i \sum_{i=1}^{N} F_{i\rightarrow j} (J_i - J_j) \quad (3)$$

Where Q is heat of radiation, W

A_i is area of surface, m^2

N is number of surfaces of the enclosure

J is radiosities

2.3.2 Heat of convection

Film temperature is used to determine thermal conductivity, kinematic viscosity of the fluid, Prandtl number and coefficient of volume expansion, which is opened from A-15 in text book of Heat and Mass Transfer Fundamentals and Applications 5^{th} Edition by Yunus A. Cengel and Afshin J. Ghaja.

$$T_f = \frac{T_s - T_\infty}{2} \quad (4)$$

Where T_f is film temperature, ºC

T_s is temperature of the surface, ºC

T_∞ is temperature of the fluid sufficiently far from the surface, ºC

The Rayleigh number for an enclosure is determined from

$$Ra_L = \frac{g\beta\,(T_1-T_2)\,L_c^3}{\nu^2}\,Pr \quad (5)$$

Where Ra_L is Rayleigh number for enclosure

g is gravitational acceleration, m/s^2

β is coefficient of volume expansion, 1/K ($\beta = 1/T_f$ for ideal gases)

ν is kinematic viscosity of the fluid, m^2/s

L_c is distance between the hot and cold surfaces, m

Pr is Prandtl number

T_1 is temperature of hot surfaces, ºC

T_2 is temperature of cold surfaces, ºC

For vertical enclosures with larger aspect ratios, Nusselt number is determined from

$$Nu = 0.42\,Ra_L^{1/4}\,Pr^{0.012}\,(H/L_v)^{-0.3} \quad (6)$$

Where Nu is Nusselt number

Ra_L is Rayleigh number for enclosure

Pr is Prandtl number

H is height from the base, m

L_v is high vertical, m

Then, heat of convection can be determined from

$$Q_{convection} = k\,Nu\,A_s\frac{(T_1-T_2)}{L_C} \quad (7)$$

Where k is thermal conductivity of material, W/m·K

Nu is Nusselt number

A_s is heat transfer surface area

T_1 is temperature of hot surfaces, ºC

T_2 is temperature of cold surfaces, ºC

L_c is distance between the hot and cold surfaces, m

2.3.3 Heat of conduction

Thermal resistance of medium depends on the geometry and the thermal properties of the medium. The thermal resistance of conduction can be determined from

$$R = \frac{L}{kA} \quad (7)$$

Where R is thermal resistance, ºC/W

L is thickness of the medium, m

A is surface area, m^2

Then, Heat of conduction can be determined from

$$Q_{conduction} = kA(T_1-T_2) \quad (8)$$

Where $Q_{conduction}$ is heat of conduction, W

k is thermal conductivity of material, W/m·K

A is surface area, m^2

R_{total} is total thermal resistance, ºC/W

In this study, the waste wax, which is in the category of fatty acid in table 1, is an interesting material to be used as PCM. The selected waste waxes are palm wax and rice bran wax, which of these two has similar properties and component compared to carnauba wax, which is a good candidate for PCM use nowadays (as shown in table 2 and 3).

Table 2 Properties of waste waxes

Property	**Carnauba wax** [16]	**Rice bran wax** [17]	**Palm wax** [18]
Melting point (°C)	84.0	76.1-82.2	46.6-53.8
Flash point (°C)	300.0	271.1	318.0
Acid value (%)	2.0-7.0	1.0-10.0	10.0-15.0
Ester value	71.0-90.0	73.0-110.0	160.9-172.8
Saponification value	78.0-95.0	75.0-120.0	190.0-202.0
Iodine value (Max)	5.0-11.0	20.0	51.0-55.0
Cost (Baht/Kilogram)	1,054	12-20	65

Table 3 Composition of natural waxes

Composition	Carnauba wax [19]	Rice bran wax [17]	Palm wax [18]
Lauric acid (C12:0)	-	-	0.20
Myristic acid (C14:0)	28.75	-	1.10
Palmitic acid (C16:0)	10.23	3.60	44.00
Stearic acid (C18:0)	11.72	2.30	4.50
Oleic acid (C18:1)	1.42	-	39.20
Linoleic acid (C18:2)	0.77	-	10.10
Linolenic acid (C18:3)	0.24	-	0.40
Arachidic acid (C20:0)	28.75	5.30	0.10
EPA (C20:5)	-	-	-
Behenic acid (C22:0)	16.75	26.10	-
Lignoceric acid (C24:0)	28.66	40.50	-
Cerotic acid (26:0)	-	11.50	-
Montanic acid (28:0)	-	6.60	-
Nonacosylic acid (29:0)	-	-	-
Melissic acid (C30:0)	-	3.10	-
Lacceric acid (C32:0)	-	1.00	-
Geddic acid (C34:0)	-	-	-

The drawback of fatty acid PCMs is low thermal conductivity. However, it can be improved by adding conductive materials. Porous material is studied due to the high thermal conductivity.

N.M.S Hidayah et al. [20] compared the properties of graphene oxide (GO) and reduced graphene oxide (rGO) with graphite to use as thermal conductivity improvement material. Improved Hummer's method [21] was used to prepare the GO and hydrazine hydrate was used to reduce GO to rGO. Graphite, GO, and rGO are porous material, which were analyzed by using Scanning Electron Microscopy (SEM) and Fourier Transform Infra-Red (FTIR). SEM was used for morphological analysis. For investigation of the functional group, FTIR was used. The experimental results showed that graphite, GO and rGO had different morphologies, functionalized groups, and crystallinity. From SEM analysis, graphite had platelet-like crystalline form of carbon and GO had the wrinkled and layered flakes on the surface. Whereas rGO had surface contained crumpled thin sheets which accumulated to form disordered structure material. Besides, the result of FTIR analysis showed the GO had presence of the plentiful oxygen-containing functional group when compared with the graphite and rGO. Therefore, reducing of GO improved porous material and properties better.

However, less performance using graphite gave compare to GO and rGO due to effect of graphite structure. Graphene oxide is film sheet of carbon 1 atom is invented to improve thermal property of PCMs. Graphene oxide has high electrical conductivity (3100-5300 W/m·K) [22, 23], high specific surface area (≈2630 m^2/g) [24], high thermal conductivity and excellent mechanical properties [25, 26]. Besides, the cost of preparation of graphene oxide is less than graphite [27]. So, graphene oxide is suitable materials for improving thermal conductivity of PCMs [28, 29].

Lin Liu et al. [30] examined effect of reduced graphene oxide (rGO) network and Ag nanoparticles on thermal conductivity of nano-enhanced phase change materials (NePCMs). First, graphite powder with specific diameters (8000 mesh) were synthesized by using modified Hummer's method [21]. This method was employed to synthesize reduced graphene oxides from graphite powder by stirring with concentrated H_2SO_4 and $KMnO_4$. From the results, 10 wt% of rGO was added to perform rGO/PCMs composite effects to thermal conductivity which has increased from 0.29 W/m·K to 3.21 W/m·K. Ag nanoparticles was applied to substitute some part of graphene to perform rGO/PCMs/Ag composite also effects to thermal conductivity which equals 5.89 W/m·K.

Wonjun Park et al. [31] formed reduced graphene oxide (RGO)/polystyrene (PS) composites by varying concentration of RGO to study electrical and thermal conductivity of composites. RGO/PS composites were produced by modified Hummers method and chemical reduction method. Raman spectroscopy was used to show increasing of electrical conductivity of RGO/PS composites when concentration of RGO was increased due to occurring conductive networks of RGO. Moreover, thermal conductivity of RGO/PS composite with 10 vol% of rGO was increased 90% when compared with pure PS. However, RGO/PS composite had thermal conductivity less than nano graphite/PS, graphite/epoxy, and graphene/epoxy composites at the same concentration due to weaker linkages between polystyrene and reduced graphene oxide.

S. Harish et al. [32] studied the preparation of lauric acid as phase change nanocomposites with graphene nanoplatelets. The thermal conductivity was measured by using transient hot-wire method. Based on their experiment results, the thermal conductivity of the phase change nanocomposites increased gradually with increasing the loading of graphene nanoplatelets. The thermal conductivity of phase change material increased 230% by adding graphene nanoplatelets of 1 vol%. In addition,

the experimental results were also compared with the model calculations based on the effective medium theory. Their experimental results showed that graphene based nanocomposites have good performance exceeding carbon nanotubes or metal nanoparticles reported in the literature. Differential scanning calorimetry results showed the insignificant change in the phase transition enthalpy and melting temperature compared to pristine lauric acid, which is measured as 181 ± 3 J/g for the PCM and the nanocomposites and melting temperature is 43.8 ± 0.1 ºC.

Chesta Ruttanapun et al. [33] synthesized nano-composited rGO-C_3AH_6 to enhance Vickers micro hardness, dielectric constant, electrochemical property, thermal conductivity, and antibacterial property. Therefore, to synthesize nano-composited rGO-C_3AH_6 with diameter of particles size 10-12 nanometers, $Ca_{12}A_{14}O_{33}$ and rGO colloid were used as substrates via rapid hydration cement process with water at 100 ºC. X-ray diffraction technique (XRD) was used to confirm $Ca_{12}A_{14}O_{33}$ can be used as substrate in C_3AH_6 hydration products. In addition, nano-composited rGO-C_3AH_6 was performed along difference concentration of dense rGO nanosheet that were loaded included 1 wt% rGO-C_3AH_6, 2 wt% rGO-C_3AH_6, 3 wt% rGO-C_3AH_6 and 4 wt% rGO-C_3AH_6 or x %rGO- C_3AH_6 (x=1,2,3 and 4). Nano-composited x% rGO-C_3AH_6 were analyzed by using Raman spectroscopy, FTIR, UV– visible spectrometer, X- ray photoelectron spectroscope (XPS), Thermogravimetric analysis (TGA), Transmission electron microscopy (TEM), and a high-resolution TEM (HRTEM). The results showed Vickers micro hardness, dielectric constant electric conductivity nano-composited rGO-C_3AH_6 were increased of when rGO content was increased. On the other hand, thermal conductivity of nano-composited rGO-C_3AH_6 was decreased when rGO-C_3AH_6 was increased in composite but enhancement of electrochemical property was occurred due to increasing of oxidation peak. And antibacterial property was demonstrated by decreasing of E.coli particle when rGO content was increased.

Warzoha et al. [34] studied effect of oriented herringbone style graphite nanofibers (HGNF), which have average diameter of 100 nm and average length of 20 μm in an organic paraffin as phase change material (PCM). HGNF were inlayed into paraffin that has melting point 56.15 ºC to perform Nanocomposite PCMs with 0.05%, 0.1%, 0.2%, 0.3%, 0.4%, 2.8%, 5.8%, 8.5% and 11.4% volume fraction of HGNF (HGNF/PCM). the Specific properties of HGNF/PCM were analyzed including thermal conductivity and latent heat as a function of temperature and HGNF volume loading

level. Thermal conductivity of HGNF/PCM composites was identified by using transient plane source (TPS) technique. In addition, latent heat of fusion and melting temperature of HGNF/PCM composites were identified by using a Differential Scanning Calorimeter (DSC). The results showed that thermal conductivity in solid phase, which was measured at 20ºC and liquid phase which was measured at 65ºC were difference. Thermal conductivity of HGNF/PCM in solid phase increases at a higher rate than liquid phase as a function of HGNF volume loading level due to a fully percolating network of HGNF does not support heat flow in HGNF/PCM in liquid phase but it supports in HGNF/PCM in solid phase. Therefore, 8.5% volume fraction of HGNF can be enhanced 180% of thermal conductivity while latent heat was decreased 10% when compared with pure paraffin.

Nurten Sahan et al. [35] performed a paraffin composites by added multiwalled carbon nanotubes and activated carbon in power form by using dispersion technique. Paraffin multiwalled carbon nanotube composite (PCNC) and paraffin activated carbon composite (PACC) were prepared in two steps including sonication and solidification by adding 1% wt multiwalled carbon nanotubes (MWCNTs) and 10% wt. activated carbon (AC), respectively. Scanning electron microscope (SEM), X-ray diffraction (XRD), Fourier transform infrared (FTIR), thermal conductivity measurement or diffusivity and conductivity (DICO) experiment and differential scanning calorimeter (DSC) were used to define effect on thermal conductivity, diffusivity and thermal energy storage capacity of paraffin composites when compared with pure paraffin. The results showed thermal conductivity of PCNC and PACC were increased 38.5% and 17.2%. Thermal diffusivity of PCNC and PACC were increased 39.1% and 34.7%, respectively. In addition, thermal energy storage capacity of PCNC was increased 9.6% while PACC was kept the same. This research showed the good results when adding additive to enhance thermal properties of phase change materials (PCMs) for thermal energy storage (TES) applications. Therefore, their novel composite oleic acid present vast potentials to stabilize the performance of the solar sorption system.

Wei Li et al. [36] investigated heat transfer performance of composite materials that were performed by adding graphite additives into phase change material. Composite phase change materials (CPCMs) were prepared by mixing expanded graphite (EG), graphene (GR) and graphene oxide (GO) in different concentration (0.5wt%, 1.0wt%, 1.5wt% and 2.0wt%) with paraffin base used as phase change

material. Compatibility of CPCMs were verified before heating and cooling of CPCMs were tested to study characteristic of charging and discharging process. In addition, T-history method was used to identify thermophysical properties of CPCMs. The results of heat charge rate showed increasing of heat charge rate depended on increasing additive concentration and CPCM with 2.0% GR was highest heat charge rate in graphite additives so heating time reduced 51.25% when compared with pure paraffin. EG was lowest heat charge rate when compared with other graphite additives. GR was also highest heat discharge rate, but heat discharge process did not affect as charge process due to heat transfer was heat convection in liquid phase. Thermophysical properties included thermal conductivity and latent heat. Thermal conductivity of CPCMs were increased when concentration of graphite additive was increased and the highest to lowest heat transfer performance was GR, GO and EG. Since graphite additives did not have latent heat so when concentration of graphite additives increased, latent heat of CPCMs were decreased as linear relation. The latent of CPCM with EG was higher than other additives because the molecular potential energy of the whole material was increased when concentration of EG increased. However, GR was the best candidate graphite additive for heat transfer enhancement although the latent heat of EG was highest.

X. Zhao et al. [37] used expanded graphite (EG) as porous additive to enhance thermal conductivity of carnauba wax (CW), which is used as phase change material (PCM). In order to identified thermal and physical properties of composite, scanning electron microscope (SEM), thermal constants analyzer (Hot Disk), differential scanning calorimeter (DSC) and Fourier transform infrared spectrometer (FT-IR) were used for analysis step. The results from analyzers showed that temperature of CW/EG composite in liquid and solid phase were 81.98ºC and 80.43ºC. Time during heating and cooling process of CW/EG composite were reduced by 81.7% and 55.3% respectively when compared with pure CW. Furthermore, thermal conductivity of CW/EG composite equaled 17.4 times of CW while latent heat during endothermic/exothermic of the CW and CW/composite were reduced by 4.96%/4.78% and 2.05%/3.44% respectively.

Nourani et al. [38] added nano-aluminium oxide (Al_2O_3) into paraffin to perform nano composite phase change material (PCM). Sodium stearoyl lactylate (SSL) was used as a surfactant for dispersion of Al_2O_3 nanoparticles in molten paraffin to mix suspension as homogenous solution by adding SSL/Al_2O_3 mass ratio 1:3.5.

Thermocouple and the transient hot wire technique are used to define properties of nano-composite PCM with 2.5, 5.0, 7.5 and 10.0 wt.% of Al_2O_3 nanoparticles were tested for melting rate at a temperature range 50-60ºC and measured thermal conductivity values in the solid and liquid phases at a temperature range 25-75 ºC, respectively. Moreover, differential scanning calorimetry (DSC) was used to identified values of melting temperature, latent heat and thermal reliability of nano composite PCM. From the results, thermal conductivity of nano composite PCM with 10 wt.% Al_2O_3 nanoparticles in the solid and liquid phases were increased 31% and 13%, respectively when compared with pure paraffin. In the same way that melting rate of nano composite PCM with 10 wt.% Al_2O_3 nanoparticles was also increased 27%. Thermal reliability was good after melted/frozen 120 cycles so can be concluded that nano composite PCM can used for thermal energy storage application.

Yang et al. [39] studied the use of nano-Si_3N_4 in order to enhance thermal performance of phase change materials (PCMs). Different mass ratios (1%, 2%, 3%, 4%, 5% and 10% by weight) of nano-Si_3N_4 were mixed with paraffin and used Ultrasound dispersion technology that makes nano-Si_3N_4 evenly distributed in paraffin to obtain nano-Si_3N_4/paraffin composite PCMs. Differential scanning calorimetry (DSC) was used in order to measure the thermal properties of PCMs and the thermal conductivities were measured by Transient Hot-Bridge method (THB-method). The experimental results showed that adding Si_3N_4 at a higher ratio causes increasing the value of thermal conductivity and thermal diffusivity. At 10 wt% Si_3N_4 additional ratio, thermal conductivity increased from 0.2293 W/m·K to 0.3090 W/m·K and thermal diffusivity increased from 0.2139 mm^2/s to 0.3137 mm^2/s that compared with pure paraffin. The thermal conductivity of composite PCMs rising by 35% and thermal diffusivity rising by 47%. Moreover, Si_3N_4 addition at higher ratio also increasing the latent heat. The latent heat of the composite PCMs was increased by 3.4% higher than using pure paraffin.

MN Mohd Iqbaldin et al. [40] studied the properties of coconut shell activated carbon (CSAC). The microwave carbonization irradiation system was used to produce activated carbon using coconut shells. The potassium hydroxide (KOH) was used as the activating agent. The surface area, pore size and specific capacitance value of the carbon produced were analyzed to investigate the potential as an electrode material for supercapacitor. The pore size and structure of the activated carbon were determined using N_2 adsorption Brunauer-Emmett-Teller (BET) and scanning electron microscope

(SEM) respectively. This process was carried out at 600 W with an irradiation time of 10 to 30 minutes. The experimental results showed that the activated carbon that was produced had a high surface area when compared with the inactivated carbon. The surface area of activated carbon produced had 1,244.0 - 1,768.8 $m^2 g^{-1}$, but the surface area of inactivated carbon biomass is only 36.5 $m^2 g^{-1}$. The pore size of the activated carbon from BET analysis was in the range of 2.3-2.9. The best activation time obtained in producing carbon material that had a large surface area (1,768.8 $m^2 g^{-1}$) and optimum porosity (2.7 nm) was at 20 min. Moreover, the specific capacitance value of the material also increased from 6.4 $F \cdot g^{-1}$ to 156.3 $F \cdot g^{-1}$ compared with the inactivated biomass.

Jin Zhequen et al. [41] studied thermal conductivity and permeability of activated carbon (AC) absorbents that were classified to three types include granular AC, consolidated AC with chemical binder and consolidated AC with expanded natural graphite (ENG). Thermal conductivity was examined by using steady state heat source method which showed thermal conductivity of granular AC was high when heating power was low therefore time reaching to equilibrium state was long. In addition, consolidated AC adsorbents were improved by smaller size of granular AC by existing of chemical binder and ENG had thermal conductivity around 0.4 W/m·K and 2.61 W/m · K, respectively. Thermal conductivity of consolidated AC adsorbents was increased 7 times when compared with granular AC. Permeability of granular AC and consolidated AC with chemical binder was better than consolidated AC with ENG due to bigger size of particles so pressure difference between two sides of testing sample close to zero.

Tumirah Khadiran et al. [42] studied the preparation of a shape-stabilized n-octadecane/ activated carbon nanocomposite phase change material for used as thermal energy storage (TES) for building applications. A one-step impregnation method was used in this application. DSC and FTIR techniques were used to evaluate changes in the thermal properties and chemical stability of the sample. Activated carbon (AC) was used as inorganic framework material and n-octadecane was used as phase change material. The n-octadecane was mixed with AC at a mass of 0.2, 0.6, 1.0, 1.2, 1.4 g. The n-octadecane/AC nanocomposites were referred to as SPCM1 , SPCM2 , SPCM3 , SPCM4 , and SPCM5 . The experimental results showed that the mass loading percentage of n-octadecane increased when octadecane/AC mass percentage ratio increased. From the results of FESEM images and nitrogen adsorption-desorption, the

n-octadecane was uniformly adsorbed into the pores of AC. The encapsulation efficiency of n-octadecane in the SPCM1, SPCM2, SPCM3, SPCM4, and SPCM5 composites was calculated based on the enthalpy from DSC to be 0.0, 0.0, 23.3, 31.9, and 42.5 wt% respectively. SPCM5 has a good latent heat storage capacity and the capability adsorption ability of AC. Therefore, SPCM5 nanocomposite was most suitable to be used as thermal energy storage material to store thermal energy. Moreover, the gypsum boards that contained the SPCM5 nanocomposite also reduced energy consumption by decreased the indoor temperature.

Atila Ertas et al. [43] examined bulk thermal conductivity of activated carbon by Adsorbed Natural Gas (ANG) tank was improved. Activated carbon was used as an adsorbent to adsorb methane in the micro-pores of the carbon for ANG storage tank that lead to high energy density capability accomplishment more than composite-reinforced pressure vessel. Fourier's Law for heat conduction was used as reference for thermal conductivity measurement method of activated carbon by using thermocouple probes to define the distribution of temperature through tank. The results showed that the bulk thermal conductivity of activated carbon from tank was slowly increased when methane was added to the tank then the bulk thermal conductivity was constant at 0.2 W/m·K for the range of pressure from 20 to 500 psia. Therefore, ANG storage application can be used this information to develop the ANG tank.

In the analysis of PCM properties, the most important parameters are latent heat and melting point, which can be determine using Differential Scanning Colorimeter also known as a DSC. DSC is a calorimeter which is used to analyze the thermal transition of a sample used to measure the energy change (exothermic or endothermic) of a sample when the temperature is increased or decreased in the controlled atmosphere. Many researchers have been using the advantage of PCMs as energy storage in different applications. The following are review of some of the recent use of PCMs.

L. Jiang et al. [44] studied a novel composite material for cold storage. Oleic acid was used as phase change material and carbon coated aluminum with different mass ratios (0.25 wt%, 0.5 wt%, and 1 wt%) were used as additive. Light flash method and viscometer were used in order to investigate the thermal conductivities and viscosities of samples. Latent heat and phase change temperature were analyzed by differential scanning calorimeters (DSC) measurements. Their experiment result showed that the thermal conductivities of composite oleic acid using nanoparticles were

improved by comparison with pure sample. The thermal conductivity of composite oleic acid increased after added carbon coated aluminum and the highest thermal conductivity equal to 0.42 W/m·K by adding 1 wt% mass ratio of carbon coated aluminum, which is 2 times higher than pure oleic acid. Dynamic viscosities decreased from 3.67 mPa s to 1.062 mPas by testing temperature at 25°C to 75°C.

Santhi Rekha et al. [45] studied the design of solar concentric parabolic cooker by added the arrangement of phase change material (PCM) in order to obtain proper heat storage system. The PCM-based domestic solar cooker was designed and analyzed for both applications of indoor and outdoor. The receiver is a hollow concentric cylinder. The inner and outer of receiver radius is about 0.09 m and 0.1 m respectively. The gap between the two layers of the receiver was filled with the heat transfer oil. The vertical cylindrical PCM tubes surrounded the outer layer of the receiver which diameter is 0.025 m and is placed at the focus of the parabolic dish. The modes of heat transfer including radiation, convection, and conduction are explained and analyzed by heat transfer network. SketchUp software is used in order to help the schematic view of the receiver. In their experiment, the performance parameters, optical efficiency factor, heat loss factor and cooking power of domestic solar cooker were calculated both with and without PCM. The experimental results showed that the heat loss factor of domestic solar cooker with and without PCM is 7.74 W/m^2 and 2.46 W/m^2 respectively. Moreover, the optical efficiency factors that presented in the receiver of domestic solar cooker with and without PCM is 0.22 and 0.098 respectively. The optical efficiency factor of domestic solar cooker that has PCM receiver is two times more than without receiver PCM. The cooking power of domestic solar cooker with PCM receiver is 125.3 W. On the other hand, the cooking power of domestic solar cooker without PCM receiver is 65.6 W. Obviously, the cooking power of domestic solar cooker with PCM receiver is more than without PCM. Thus, the design of PCM solar cooking system can widen the applicability of domestic solar cookers and It is a cooking solution that is compatible for cooking applications instead of cooking systems using fossil fuels.

Anderson et al. [46] studied the latent heat storage system by using coconut oil as phase change material (PCM). Hot water tank used as latent heat storage box was designed and improved. The hot water tank was divided into two parts including part of cold water containing that with inlet and part of spiral tube containing surrounded by PCM. The water was used as heat transfer at the flow rate is 2 kg/min. In their

study, the hot water tank was fabricated by ANSYS software in order to perform analysis. The average temperature of hot water for the thermal energy storage system was developed at 60ºC. The charging and discharging process was obtained from this experiment by plot the relation between temperature (ºC) and time (min).

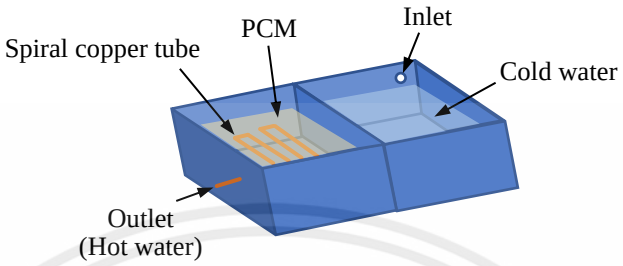

Figure 1 Latent heat storage box [46]

The experimental results showed that design analysis gave good results in the ANSYS modeling. From investigation, the temperature of hot water can be increased by using PCMs arrangement in the tank with copper tube. The tank consists of copper tube and PCM reduced heating time by 16% compared with the hot water tank without PCM. Therefore, the application of PCM in a hot water tank has good potential for storing latent heat and can be used in solar water heating applications.

Kanyarat Holasut et al. [14] studied the solar dryer in order to increase the period of the heat stored energy in a limited portion of time during maximum solar radiation by incorporating a suitability phase change materials (PCMs). The temperature required to keep inside solar dryer was around 40ºC. The solar dryer has a capacity of 2.5 m^3. The 40 kg of phase change material was placed under the solar collector panel in order to supply the electricity when necessary. Paraffin wax was used as the phase change material and mixed with kerosene in ratios of 1:1, 2:1, 3:1 and 4:1 to compare the emission and absorption of thermal energy. The experimental results showed that the ratio of paraffin wax and kerosene of 2 : 1 could achieve the melting temperature at about 40 ºC of PCM as required. The PCM could help keeping the temperature inside the solar dryer at 40ºC for 8 hours. Therefore, PCM could improve the efficiency of the dryer by reducing the electrical energy used such as heater by 8.02%.

Jan Fort et al. [47] prepared composite phase change material for energy saving in the building industry. In order to save cost, vacuum impregnation method was used to prepared composite by using palm wax was chosen as phase change material to mix

with diatomite powder. The FTIR spectroscopy was used to determine ability to disperse of palm wax and diatomite in composite structure. In addition, DSC analysis was used to define melting point and latent heat of composite phase material. And the laser diffraction- based device was used to assign appropriate distribution of particle size. The results showed melting point and latent heat of composite phase change material were 55.95ºC and 78.0 J/g, respectively that was suitable for materials used in building application.

Helm et al. [48]applied Calcium Chloride Hexahydrate ($CaCl_2 \cdot H_2O$) as a PCM in order to store latent heat in dry air cooler of absorption cooling system. The phase change temperature of PCM was 29ºC was applied to absorb 50% of the daily reject heat load. In addition, latent heat was stored in PCM could be used to ensure the temperature of cooling water at 32ºC in dry air cooler before sent to chiller.

Similarly, Helm et al. [49] also published the similar research compared the solar cooling system with traditional wet cooler water. The results showed the positive effect on the Seasonal Energy Efficiency Ratio (SEER) could be cooled up to 11.4. The absorption chiller could produce 22% of waste heat to disperse to ambient air at 30ºC.

After we harvest the energy in form of heat, we want to produce electrical charge from heat. The related theory is seebeck effect.

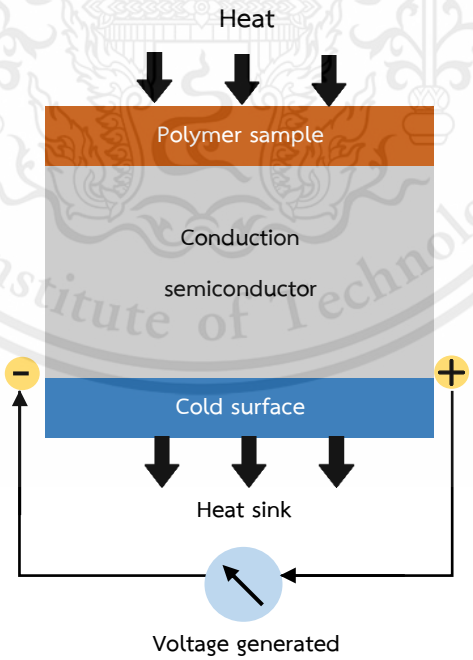

Figure 2 Semiconductor thermocouple seebeck effect [50]

The seebeck effect is phenomena that voltages can be produced from the difference of temperature between heated surface and cold surface. From Figure 2, heated electrons from heated surface are flowed to cold surface due to application of two conductors or semiconductors that are jointed with heated surface and cold surface.

In order to increase the output voltages, seebeck effect devices are connected in series whereas the maximum deliverable can be increased if devices are connected in parallel. However, the high voltage and current are provided if difference of temperature between heated surface and cold surface is large enough.

Datta et al. [51] developed a thermoelectric energy harvesting prototype for asphalt pavement. In order to generate electricity from thermal energy in pavements, the prototype of thermoelectric energy harvesting system was considered through finite element analysis, laboratory testing and field experiments. The results represented that the largest temperature could be achieved from thermoelectric generator (TEG) module with depth at 180 millimeters by using copper plate was 16 ºC. The average energy output from lab test was 1.67mW/ºC and the range of the power output was 4 mW to 6.5 mW. In addition, the authors showed the material costs of the prototypes with two and four TEGs were $190 and $94.

From the reviews of previous works, this study will show the possibility of using waste wax (palm wax and rice bran wax) as PCMs and the thermal conductivity property will be improved by addition of activated carbon and reduced graphene oxide. Moreover, the CPCM will be used in a designed portable device of thermal to electricity.

CHAPTER III
RESEARCH METHODOLOGY

3.1 Chemicals and Equipment

3.1.1 Chemicals

1. Paraffin wax
2. Palm wax
3. Rice bran wax
4 Carnauba wax
5. Reduced graphene oxide (rGO)
6. Activated carbon (AC) from coconut shell
7. Vegetable oil
8. Tap water

3.1.2 Equipment

1. Differential Scanning Calorimeter (DSC)
2. Thermal Conductivity Analysis (TCA)
3. Scanning Electron Microscope (SEM)
2. Digital magnetic hotplate stirrer
3. Ultrasonic bath
4. Analytical balance (2 digits)
5. Balance for approximate weighing (4 digits)
6. Thermocouple which type K
7. Breaker
8. Test tube
9. Glass rod
10. Stand and clamp
11. Digital magnetic hotplate stirrer

3.2 Method

3.2.1 Improvement of thermal conductivity of PCM

3.2.1.1 Selection of suitable PCM

1. Weight and record the test tube. Then, calibrate analytical balance and take paraffin wax (or palm wax or rice bran or carnauba wax) 5 g as PCM into the test tube.

2. Set the temperature of 500 mL oil heating medium at 85 °C and water-cooling medium at 30°C by using digital magnetic hotplate stirrer at the rate of 750 revolution per minute (rpm) and 500 rpm respectively.

3. Heat the test tube with PCM until wax is melt in an oil bath and set up the thermocouple into the melted PCM. Melt the PCM until the temperature is constant. Then, take of sample test tube fill with wax and let it cool down in the water bath until it crystalline into solid.

4. Measure and record the height of PCM in the solid phase in the test tube. Then, heat the PCM in the heating medium. Record the temperature of PCM every minute until the temperature is constant. (Note: Observe when the PCM begins to melt and completely melts, the temperature and height is recorded.)

5. When the temperature is constant, the height of melted PCM is measured and recorded. The test tube filled with PCM is taken off the oil bath.

6. Melted PCM is cooled in cooling medium until the temperature is constant. Record the temperature of PCM every minute. The height and weight of cold PCM immediately, after 30 minutes and after 1 hour is recorded.

7. Plot the relation between time and temperature to get charge and discharge graph.

3.2.1.2 Usage additive to enhance thermal conductivity

3.2.1.2.1 Additive section

1. Scan high resolution images of reduced graphene oxide and activated carbon by using Scanning Electron Microscope (SEM)

3.2.1.2.2 CPCM section

1. Weight and record the test tube. Then, calibrate analytical balance and take chosen PCM 5 g into the test tube.

2. Set the temperature of 500 mL water heating medium at 85 °C and water-cooling medium at 30°C by using digital magnetic hotplate stirrer at the rate of 750 rpm and 500 rpm respectively.

3. Heat PCM until melt and add reduced graphene oxide (0.5 wt%) and activated carbon (0.5 wt%, 1.0 wt%, 1.5 wt%, 2.0 wt%, and 2.5 wt%). Then, PCM is stirred at 700 rpm for 1 hour. The mixed PCM is put into the ultrasonic bath to continue mixing for 3 hours until the mixture is mixed as homogeneously.

4. The composite phase change material (CPCM) is analyzed by using Differential Scanning Calorimeter (DSC) to measure of the latent heat and melting point. And CPCM is also analyzed by using Thermal Conductivity Analysis (TCA) and Scanning Electron Microscope (SEM) to measure thermal conductivity and dispersion of CPCM respectively.

5. Set up the thermocouple into the melted CPCM from step 3. Melt the PCM until the temperature is constant. Then, take of sample test tube fill with wax and let it cool down in the water bath until it crystalline into solid.

6. Prepare the CPCM same as in step 4-7 in part 3.2.1

7. Compare the results with other samples from part 3.2.1

3.2.2 Experimental setup of prototype of a portable device

1. Attach thermoelectric power generators (peltiers) to device as the series circuit by using silicone to hot side of peltiers.

2. Connect a DC to DC converter with peltiers to convert electric power.

3. Attach heat sinks to cool side of peltiers to disperse heat by using silicone.

4. Cover insulator around device to reduce heat loss.

5. Attach computer fans to heat sinks to disperse heat from device (can we use with battery).

5. Add hot charcoal into a half of device then it will start to generate the electricity.

6. Measure temperature at hot side and cool side by using thermocouple type K.

7. Record time until the temperatures of hot side and cool side are equal.

8. Add composite PCM (CPCM) to PCM container then prepare the experiment setup same as in step 5-7.

9. Compare the results between with and without CPCM.

Figure 3 Experiment setup

3.2.2.1 Device specifications

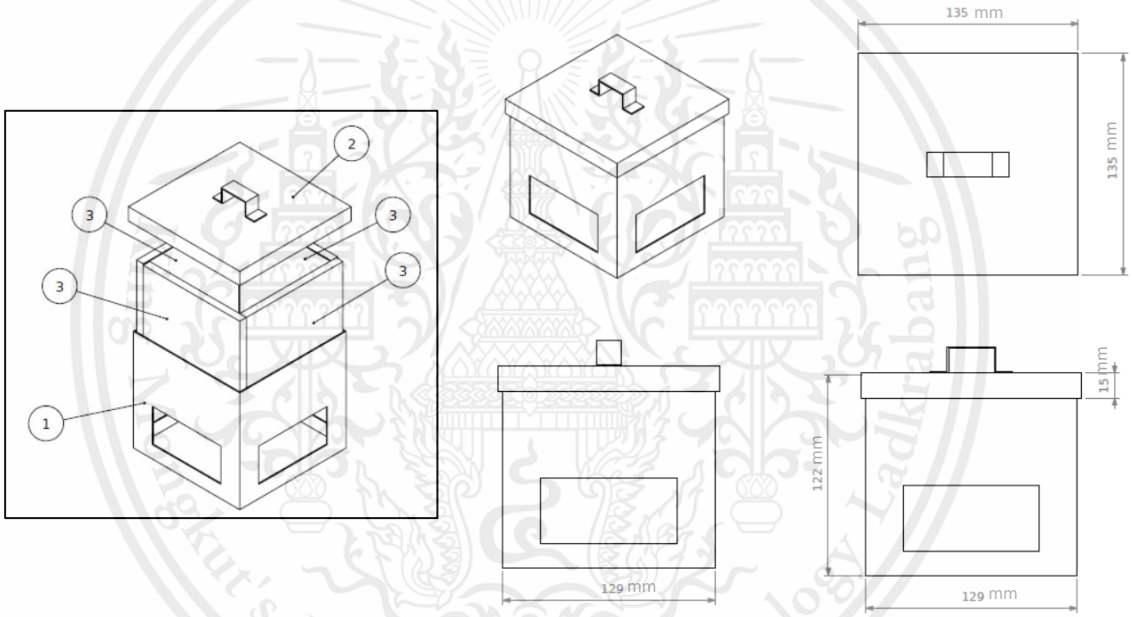

Figure 4 Device specification

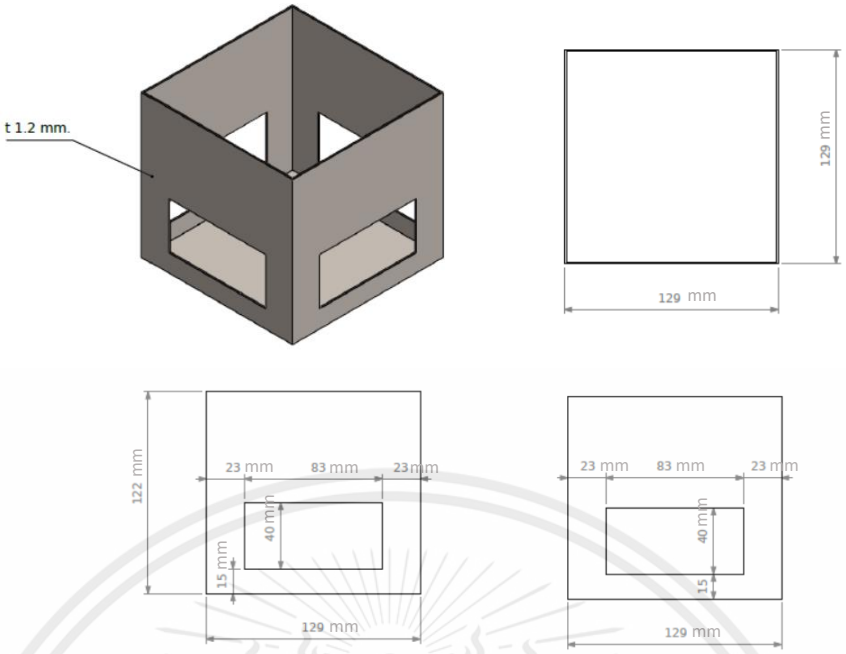

Figure 5 Specification of outer casing of PCM container

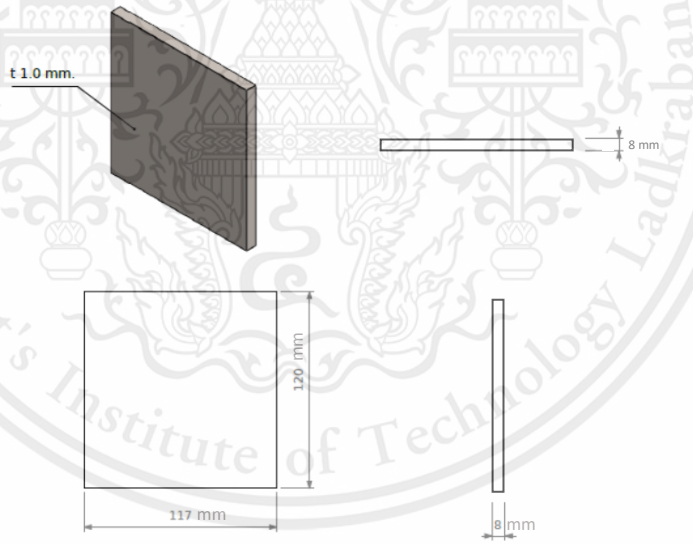

Figure 6 Specification of PCM container

CHAPTER IV
RESULTS AND DISCUSSION

4.1 Improvement of thermal conductivity of PCM

4.1.1 Selection of suitable PCM

Suitable properties of PCM for thermal energy storage (TES) application consist of high phase change enthalpy, less volume change and high thermal conductivity. From Table 4 showed the phase change enthalpy of palm wax and rice bran wax were high and the melting point of palm wax and rice bran wax were low therefore palm wax and rice bran wax were good candidates for using to enhance thermal conductivity.

Table 4 Temperature (ºC) and latent heat of waste wax (J/g) of phase change material

Waste wax	**T_m (ºC)**	**ΔH (J/g)**
Paraffin	47-65	176
Palm	40±0.339	197.31±0.160
Carnauba	82	168.3
Rice bran	48-66	197.95

Phase change enthalpy and thermal conductivity can be observed from charging and discharging cycle of PCMs that time for charging process should be low to obtain higher storage capacities in latent heat storage process. In addition, charging and discharge cycle of PCMs can be used to observe thermal conductivity due to heat transfer coefficient of heat exchanger is provided by the thermal conductivity of PCM. The results showed that palm wax is waste material that can be used to create CPCM to consume with TES application since time of charging and discharge are low is shown in Figure 7.

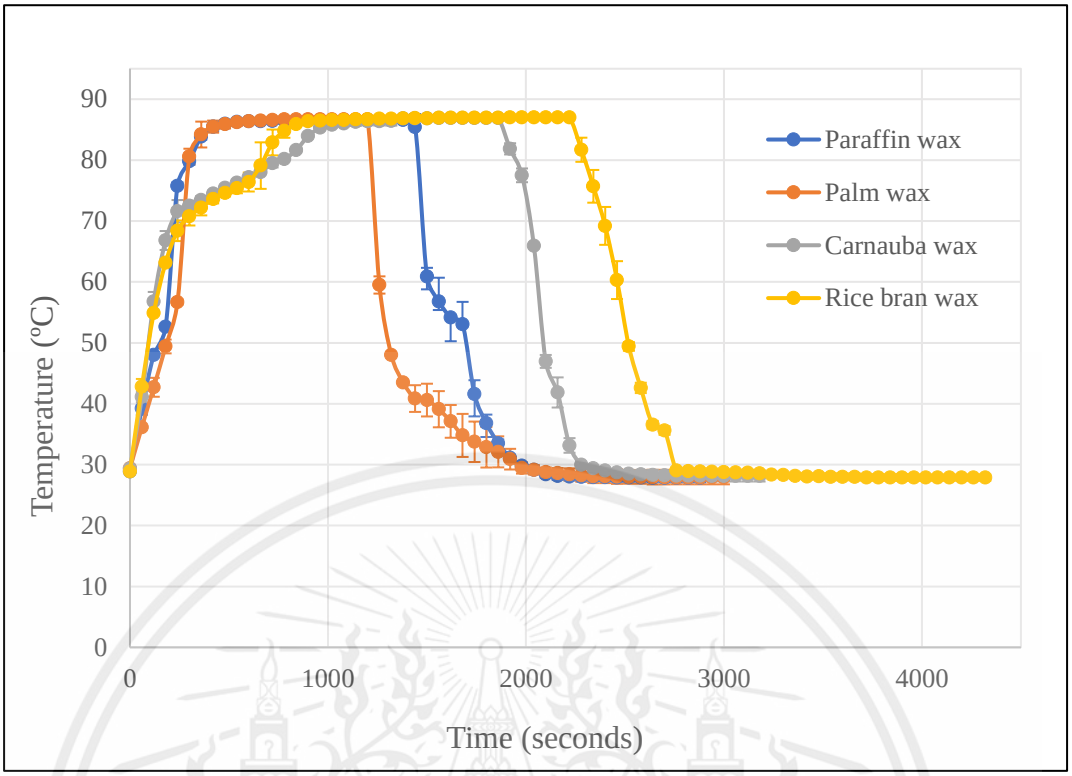

Figure 7 The relation between temperature (°C) and time (seconds) of charging and discharging cycle

Table 5 Percentage of volume change of PCMs

PCMs type	%Volume change
Paraffin wax	6.59±0.03
Palm wax	7.32±0.01
Carnauba wax	7.23±0.04
Rice bran wax	8.33±0.06

From Table 5, each of the samples were repeated 2 times. the percentage of volume after charging and discharging cycle that is increased due to expansion during phase transition of PCMs. However, percentages of volume change of paraffin wax, palm wax, rice bran wax and carnauba wax were very similar. The volume of organic PCMs change less than 10%. Thus, the effect on volume change of organic PCMs is insignificant.

Table 6 Cost (baht) of waste wax

Waste wax	Cost (baht/kg)
Paraffin	145
Palm	65
Carnauba	1054
Rice bran	20

However, the phase change enthalpy of PCMs should be ensure by DSC before the suitable PCM will be chosen because of the phase change enthalpy is required to apply with TES application. In order to obtain reasonable cost, waste waxes are focused due to cost of palm wax and rice bran wax were showed in Table 6 which are less expensive than paraffin and carnauba wax. Therefore, rice bran wax and palm wax are analyzed by using DSC.

Table 7 Latent heat of fusion of rice bran wax and palm wax

PCMs type	**Latent heat (J/g)**
Rice bran wax	197.95
Palm wax	197.31

From analyzation of DSC, the latent heat of rice bran wax is 197.95 J/g and latent heat of palm wax is 197.31 J/g. Latent heat of rice bran wax is more than palm wax. However, rice bran wax has phenomena of superheating and subcooling that lead to delaying phase change and occurring hysteresis in charging and discharging cycle which is showed in Figure 8. Comparison of pure rice bran wax and palm wax from DSC thermograms, the results showed that palm wax does not have phenomena of superheating and subcooling, therefore palm wax is chosen to use as CPCM.

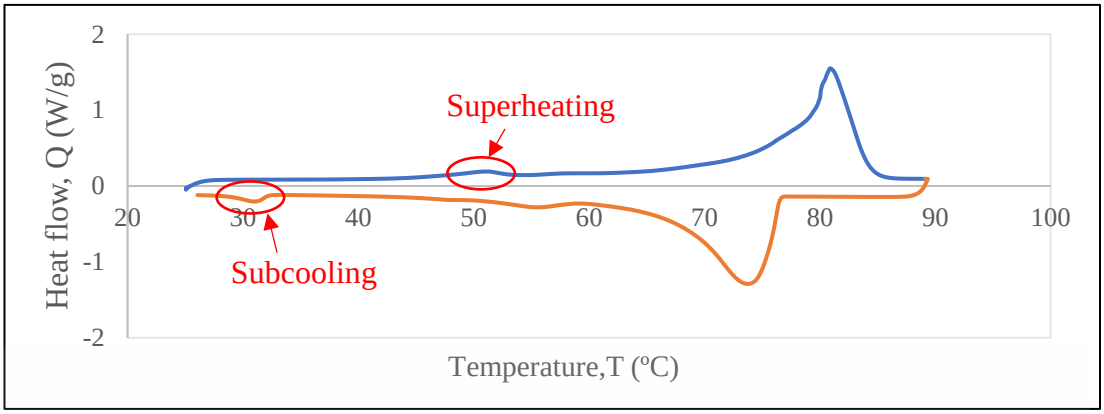

(a)

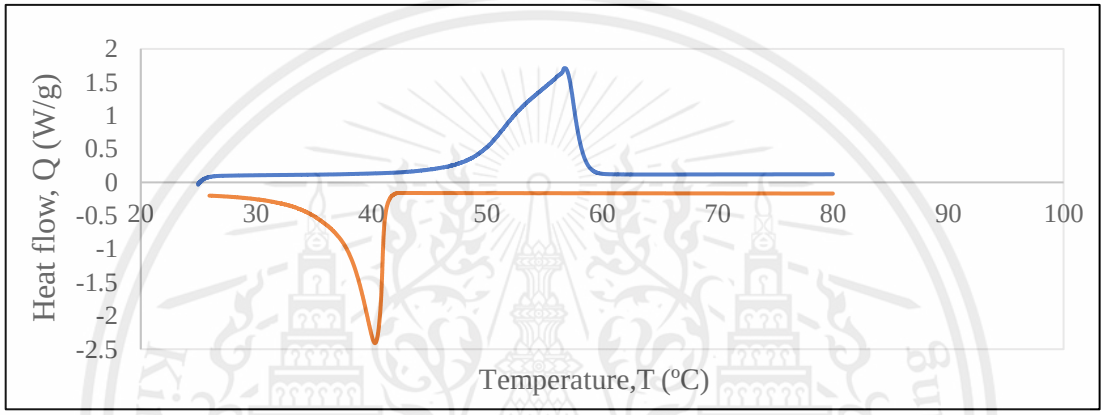

(b)

Figure 8 DSC thermograms (a) Pure rice bran wax (b) Pure palm wax

4.1.2 Usage additive to enhance thermal conductivity

In order to enhance thermal properties of PCM, additive was used to prepare CPCM which rGO and AC were chosen in this work due to widely used and high thermal conductivity. CPCM was analyzed by using SEM, charging, and discharging cycle, DSC, and TCA to apply with TES application.

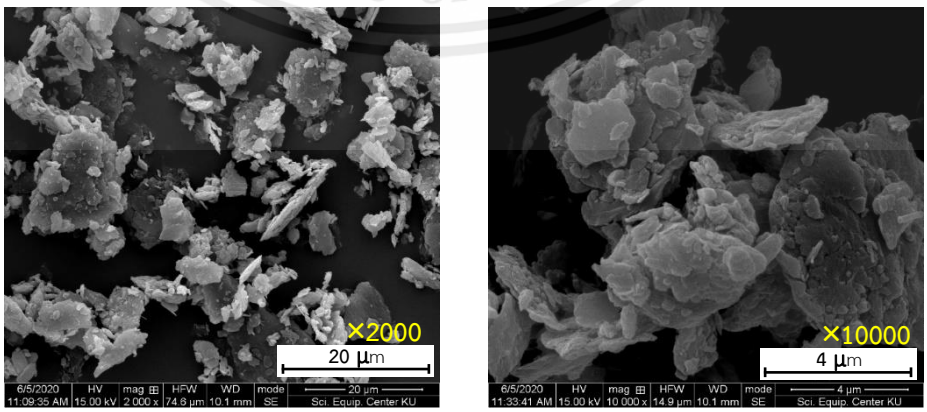

Figure 9 SEM analysis of rGO

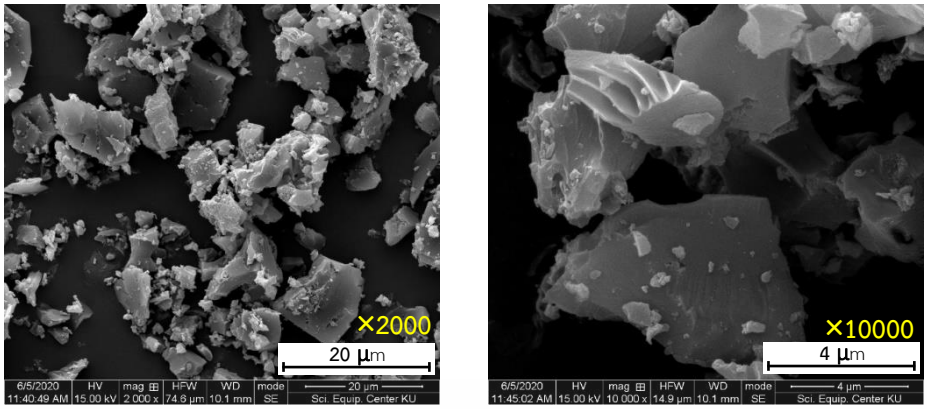

Figure 10 SEM analysis of AC

From Figure 9, rGO can be derived from graphene that includes oxygen functional groups. In addition, all carbon atoms in the structure of rGO are bonded to three neighbors maintaining a planar sp^2 configuration so rGO has good conductive properties [20]. However, disadvantages of rGO are expensive and taking a long time to synthesize.

From Figure 10, AC has amorphous structure and highly porous on structure which can be defined as a crude form of graphite. AC can be derived from a raw material that contains high percentage of carbon. The basic chemical structure of activated carbon is closely approximated by the structure of pure graphite, so AC has good conductive properties. AC can be derived easily more than rGO and has reasonable cost. In addition, Table 8 showed the similarity latent heat and thermal conductivity of CPCM with 0.5% wt of RGO and AC. Thus, AC is a good candidate for conductivity enhancement applications.

Table 8 Comparation of 0.5%wt rGO and 0.5% wt AC

0.5% wt	Latent heat (J/g)	Thermal conductivity (W/m·K)
rGO	185.98 ± 0.074	0.228 ± 0.002
AC	192.09 ± 0.164	0.216 ± 0.094

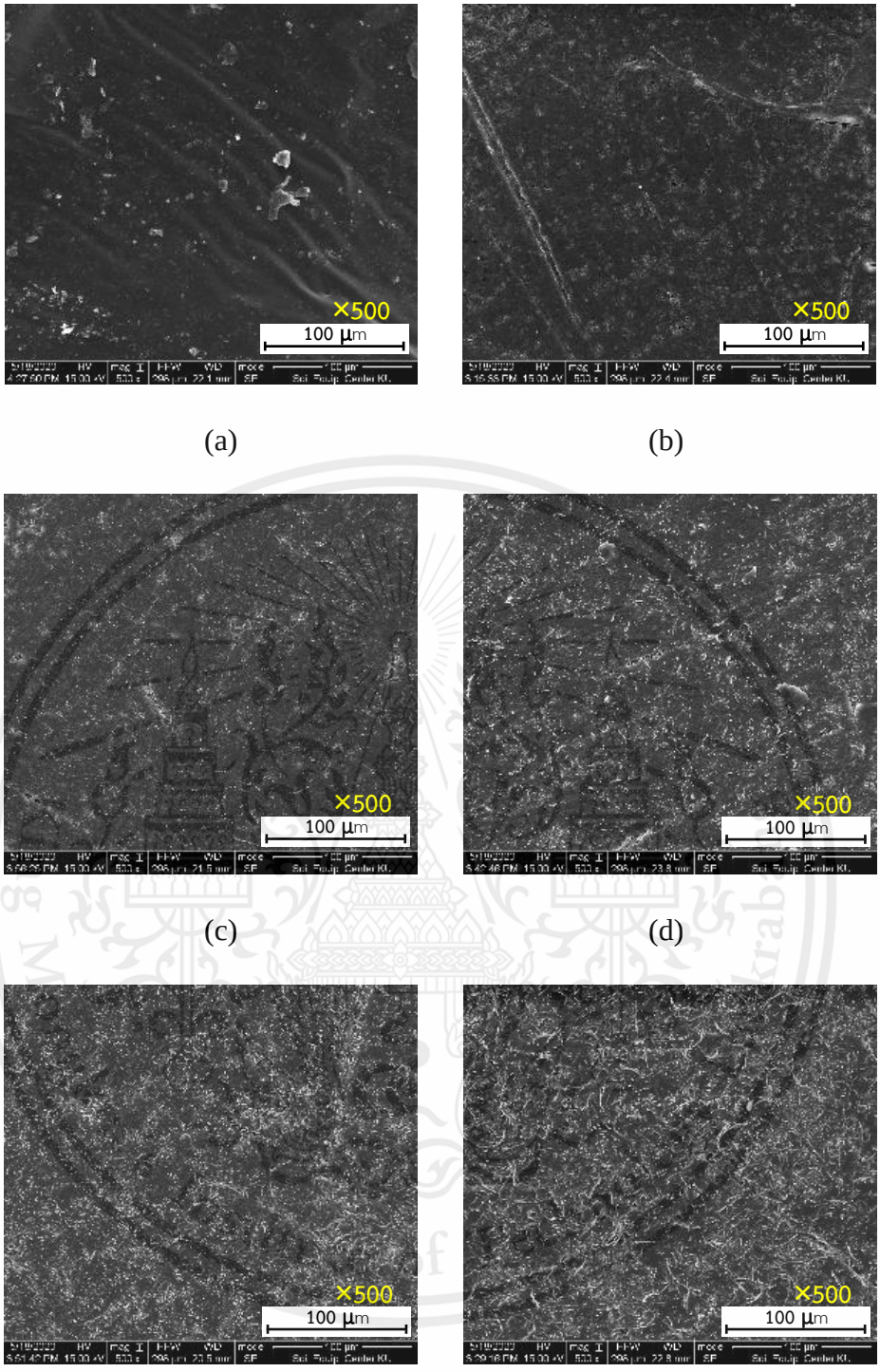

Figure 11 SEM analysis of CPCMs

(a) 0.5 wt% rGO (b) 0.5 wt% AC (c) 1.0 wt% AC

(d) 1.5 wt% AC (e) 2.0 wt% AC (f) 2.5 wt% AC

From Figure 11 (a) and (b) showed that the compatibility of 0.5 wt% AC in CPCM was better than 0.5 wt% rGO in CPCM. And distribution of AC is increased depend on concentration of AC in CPCM is increased which was showed in Figure 11 (b)-(f). In addition, results of Energy Dispersive X-ray Spectrometer (EDS) showed when concentration of AC in CPCM is increased, quantity of carbon (C) and oxygen (O) percentage by weight in CPCMs are increased and decreased, respectively due to carbon content from AC which is showed in Figure 12 and 13 respectively. Thus, SEM analysis can be indicated compatibility of AC and palm wax and good distribution of AC in preparation of CPCM.

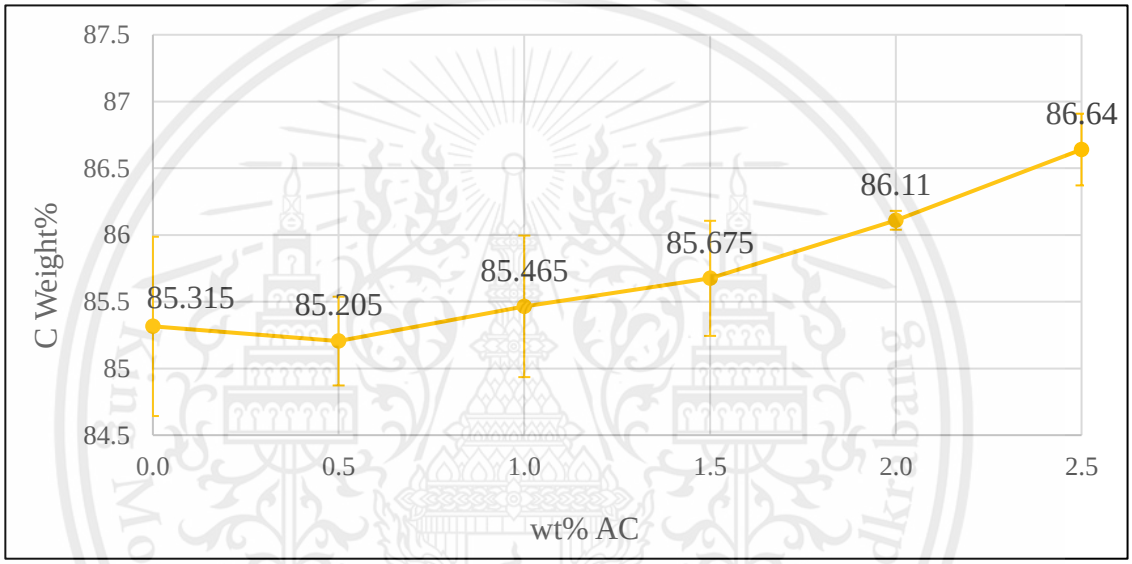

Figure 12 The relation between percentage of carbon (C) by weight and percentage by weight (%) AC in CPCMs

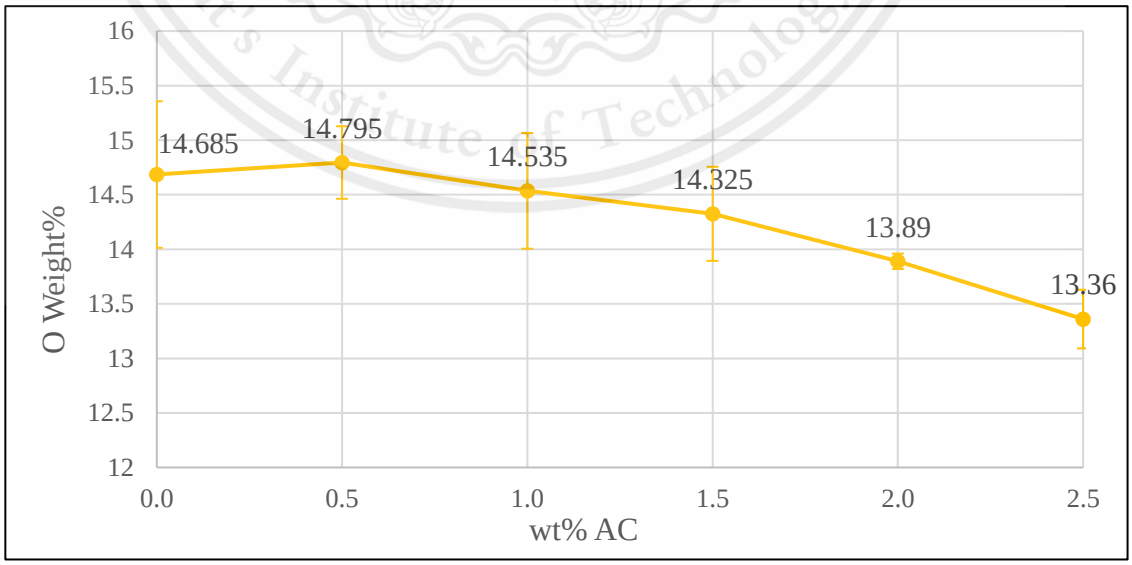

Figure 13 The relation between percentage of oxygen (O) by weight and percentage by weight (%) AC in CPCMs

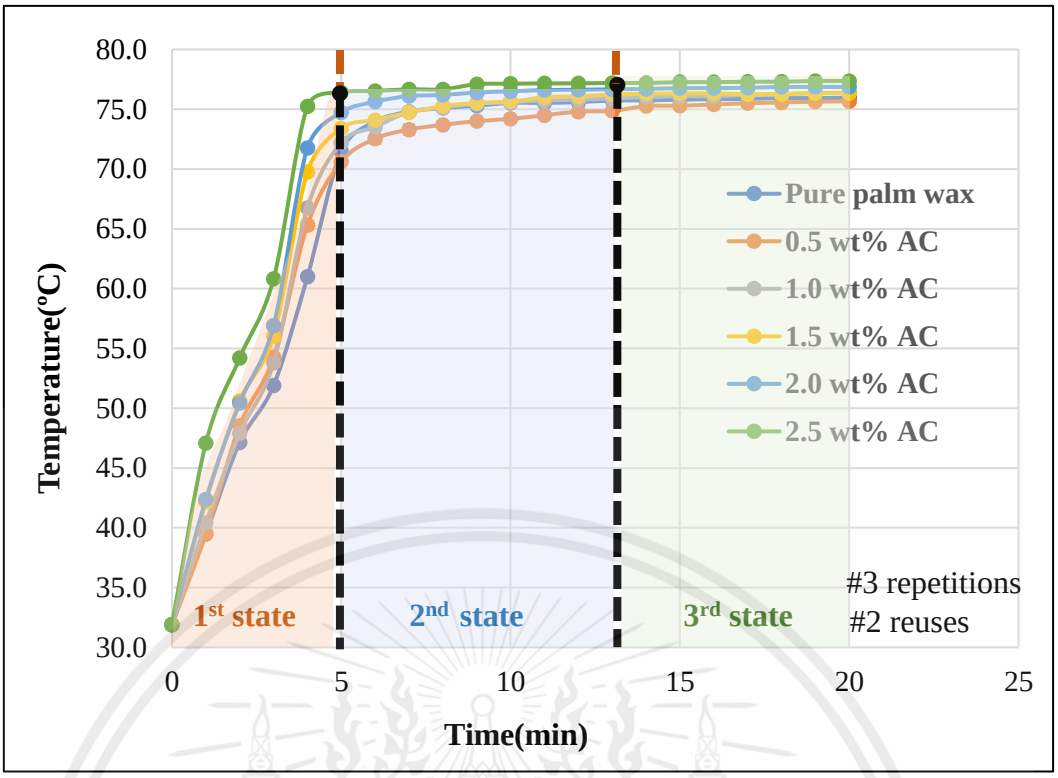

Figure 14 The relation between temperature (ºC) and time (min) of charging cycle

From Figure 14, each of the samples were repeated 3 times and reused 2 times for charging cycle which the error from testing was less than 30%. The temperature of charging cycle was divided into three stages. At first stage, the temperature increased rapidly to melting point in linear relation. Domination heat transfer of this stage was appeared only conduction.

The temperature at second stage was gradually increased due to CPCMs started melting at second stage until completely melt to liquid phase. Domination heat transfers of this stage were natural convection and conduction.

The temperature of complete melted CPCMs at third stage was slowly increased since natural convection of melted CPCMs but viscosity of CPCMs was also increased due to addition of AC. Therefore, natural convection of this stage depended on viscosity of AC in CPCMs.

From this experiment, higher concentration of AC will improve charging rate and thermal conductivity of CPCMs.

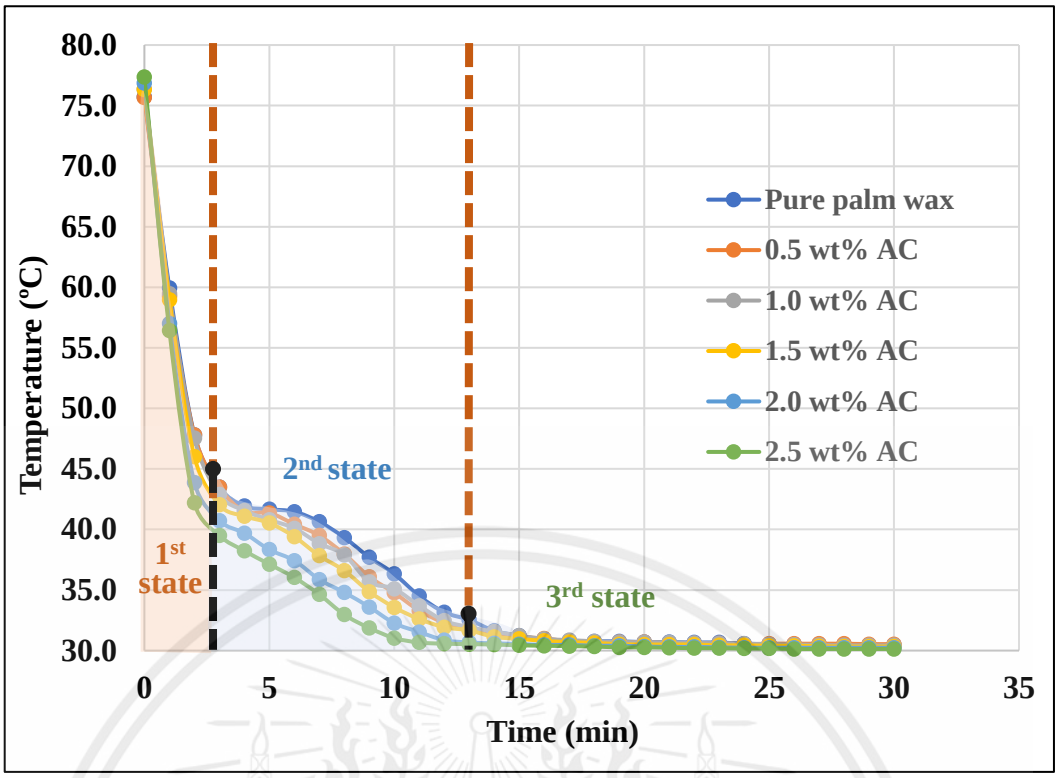

Figure 15 The relation between temperature (°C) and time (min) of discharging cycle

From Figure 15, each of the samples were repeated 3 times and reused 2 times for discharging cycle which the error from testing was less than 30%. The temperature of discharging cycle was divided into three stages.

At first stage, temperature was rapidly decreased but discharging speed of each CPCMs were similar because the large heat transfer area and the temperature difference and AC was not affected in liquid phase of CPCMs. Then, domination heat transfer of this stage was convection. The temperature at second stage was gradually decreased when CPCMs change to solid stage due to latent heat was released from CPCMs. Discharging speed at third was more rapid when CPCMs were completely solid. Therefore, domination heat transfer of this stage is appeared only conduction.

From this experiment, higher concentration of AC will improve discharging rate and thermal conductivity of CPCMs.

Table 9 Percentage of volume change of CPCMs

% By weight	%Volume change
0.0 AC	2.47±0.004
0.5 AC	3.33±0.047
1.0 AC	2.04±0.029
1.5 AC	1.82±0.026
2.0 AC	0.862±0.012
2.5 AC	2.68±0.038

From Table 9, each of the samples were repeated 3 times and reused 2 times for charging and discharging cycle. The percentage of volume after charging and discharging cycle was increased due to expansion during phase transition of CPCMs. However, percentages of volume change of CPCMs were very similar. The volume of organic PCMs changed less than 5%. So, the effect on volume change of CPCMs was insignificant.

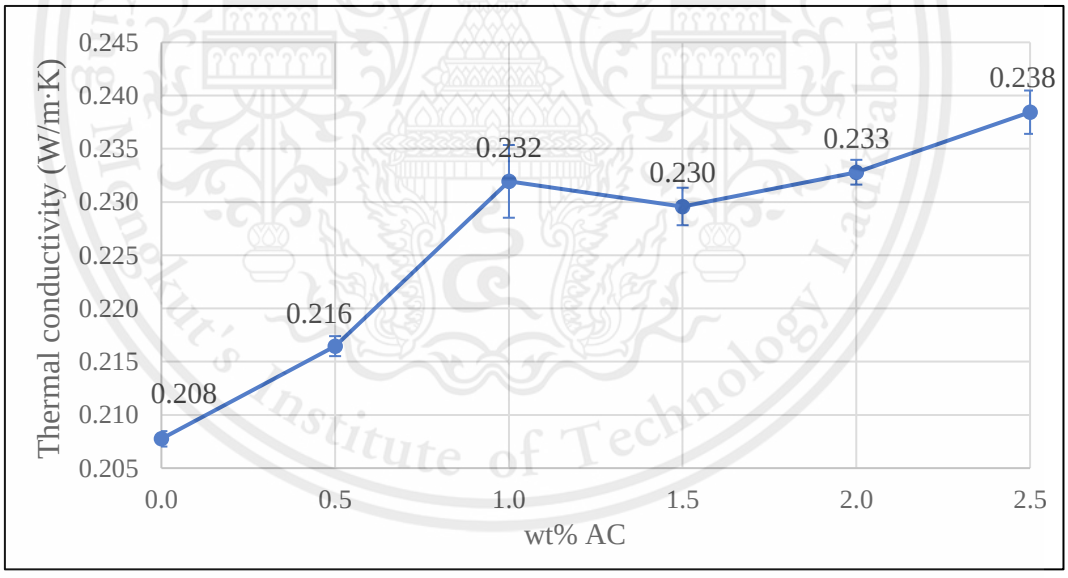

Figure 16 The relation between thermal conductivity (W/mK) and percentage by weight (%) AC

From TCA analysis, each of the samples were repeated 5 times which the error less than 0.35%. Thermal conductivity of CPCMs was plotted in Figure 16. The trend of thermal conductivity was increased depend on increasing of concentration of AC by weight due to high conductivity of AC. Therefore, 2.5 wt% of AC in CPCM could be enhanced 14.42% of thermal conductivity when compared with pure palm wax.

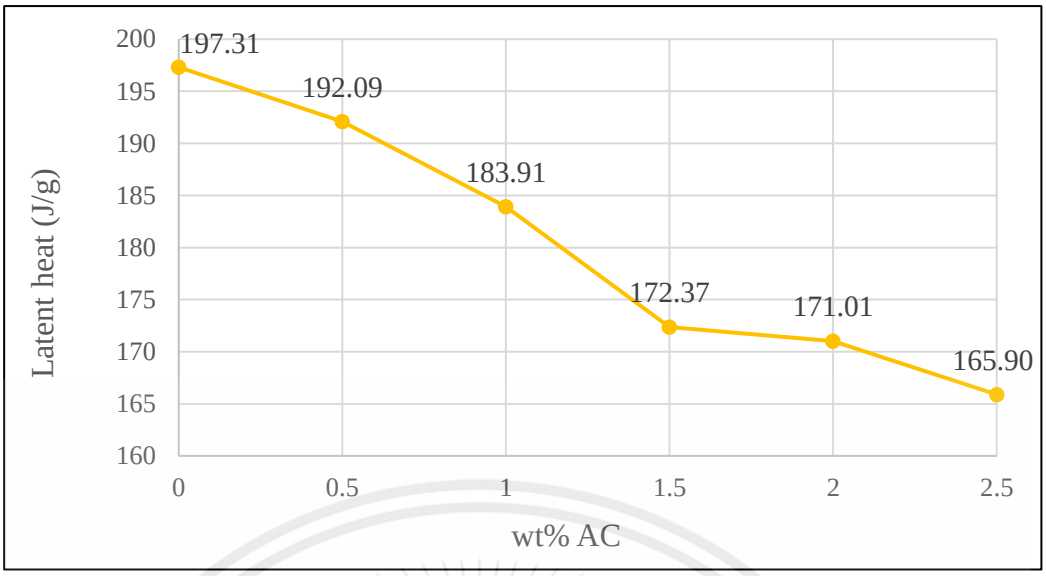

Figure 17 The relation between latent heat (J/g) and percentage by weight (%) AC

From DSC analysis, latent heat of CPCMs is plotted in Figure 17. The trend of latent heat was decreased depend on increasing of concentration of AC by weight due to AC additive does not have latent heat. Therefore, 2.5 wt% of AC in CPCM could be decreased 15.92% of latent heat when compared to pure palm wax.

The 2.5 wt% of AC in CPCM was chosen for CPCM preparing to use in TES application because high thermal conductivity and acceptable reducing of latent heat.

4.2 Experimental setup of prototype of a portable device

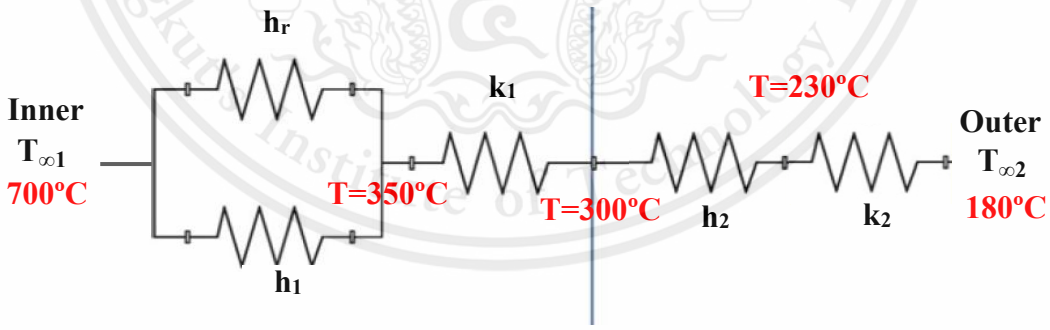

Figure 18 Heat transfer network of device without CPCM (side view)

The heat from inner device ($T_{\infty 1}$) was transferred to outer device ($T_{\infty 2}$) in the form of three modes. Includes radiation, convection, and conduction. From Figure 18, the heat from inner device ($T_{\infty 1}$) was transferred to CPCM container by radiative and convective heat transfer modes. The radiative and convective heat transfer resistances were represented as h_r and h_1 in the heat transfer network.

As the inner part of device was inserted by CPCM container, the mode of heat transfer related between the outer wall of CPCM container and inner was conduction and denoted by k_1. The heat was transferred to the whole empty inside the container by convection was represented by h_2. The heat was transferred from the wall of CPCM container to outer layer of device by conduction and represented as k_2.

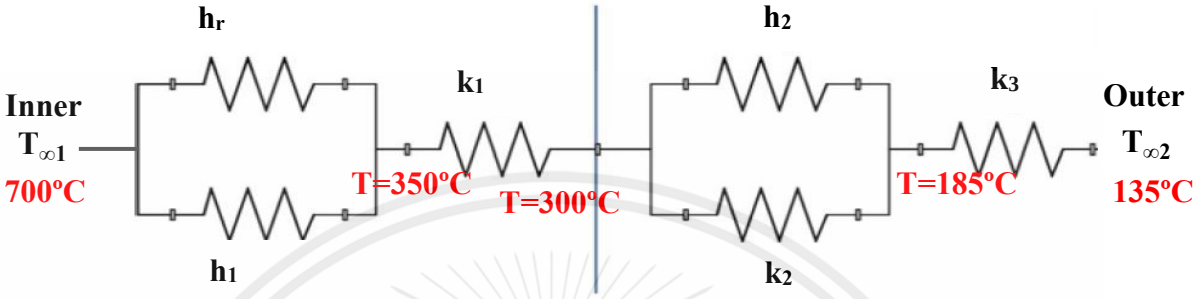

Figure 19 Heat transfer network of device with CPCM (side view)

The heat from inner device ($T_{\infty 1}$) is transferred to outer device ($T_{\infty 2}$) in the form of three modes. Includes radiation, convection, and conduction. From Figure 19, the heat from inner device ($T_{\infty 1}$) was transferred to PCM container by radiative and convective heat transfer modes. The radiative and convective heat transfer resistances were represented as h_r and h_1 in the heat transfer network.

As the inner part of device was inserted by PCM container, the mode of heat transfer related between the outer wall of PCM container and inner was conduction and denoted by k_1. The heat was transferred to the whole PCM inside the container by convection and from the last layer of the PCM to PCM wall heat was transferred by conduction that were represented by h_2 and k_2 respectively. The heat was transferred from the wall of PCM container to outer layer of device by conduction and represented as k_3.

Table 10 Comparison time of device operate without CPCM and with CPCM

Time (min)			
Start operating		End operating	
Without CPCM	With CPCM	Without CPCM	With CPCM
4.97±0.457	8.07±0.326	93.00±3.464	171.80±5.540

From Table 10, the experimental was repeated 5 times and divided into two cases including without CPCM and with CPCM. In case of without CPCM, the

electrical was started to release from device at around 5 minutes after hot charcoal was added to device. And electrical was stopped to operate at around 93 minutes after temperature at hot side and cool side were equaled. In addition, power of portable device from calculation without CPCM was equaled to 80.9 kW.

On the other hand, the electrical was started to release from device with CPCM at around 8 minutes after hot charcoal was added to device because of CPCM was not completely melt at the initial, therefore the started time to release of electrical was slower than device without CPCM. And electrical was stopped to operate at around 172 minutes after temperature at hot side and cool side were equaled which time of released electrical with CPCM was longer than without CPCM since CPCM gradually releases heat to peiltlers. In addition, power of portable device from calculation with CPCM was equaled to 81.4 kW. From the started, temperature of hot charcoal was average 700 °C for without and with CPCM for portable device application.

Therefore, from Table 10 showed 45.9% of time enhancement of portable device with CPCM when compared with portable device without CPCM.

CHAPTER V
CONCLUSION

5.1 Conclusion

The work presented heat transfer from a portable device with composite phase change material to produce electricity from natural heat. The waste wax was used as phase change material was improved and applied in the portable device. In the selection of suitable PCM part, charging and discharging cycle were used to predict latent heat and thermal conductivity of PCM. The results from DSC analysis showed palm wax and rice brane wax have similar latent heat but superheating and subcooling phenomena existed in rice bran wax. Therefore, palm wax was chosen as PCM to further improve the thermal conductivity.

Thermal property enhancement of PCM, both rGO and AC have good conductive properties, but AC was less than expensive. Thus, AC was chosen as an additive. CPCMs were prepared from palm wax/AC composite at varied percentage by weight 0.0 wt%, 0.5 wt%. 1.0 wt%, 1.5 wt%, 2.0 wt% and 2.5 wt% of AC in CPCM. CPCMs were analyzed using SEM, charging and discharging time, TCA and DSC.

In order to apply with TES application, 2.5 wt% of AC in CPCM was chosen because 14.42% of thermal conductivity enhancement when compared to the pure palm wax (k of pure palm wax= 0.208 W/mK, 2.5 wt% of AC in CPCM =0.238 W/mK). The latent heat from DSC analysis of 2.5 wt% of AC in CPCM decreased 15.92% of latent heat when compared with pure palm wax (Latent heat of pure palm wax= 197.31 J/g, Latent heat of 2.5 wt% of AC in CPCM = 165.90 J/g). SEM showed good dispersion and compatibility of AC in CPCMs. In the experimental setup of the prototype of portable device part, the portable device was tested by recording time when electrical was released from device which portable device with CPCM could be enhanced 45.9% when compared with the portable device without CPCM (portable device without CPCM = 93 minutes, portable device with CPCM = 172 minutes). Moreover, the power (Q) from calculation of device without CPCM and with CPCM were 80.9 kW and 81.4 kW respectively. However, the portable device with CPCM is still taking a started time to heat CPCM which this problem should be improved in the future.

5.2 Suggestions

1. Other waste wax should be studied to find optimum phase change material that suitable for TES application.

2. Other high thermal conductivity material should be studied to enhance thermal conductivity that suitable for TES application.

3. The portable device should be created smaller and lighter than this prototype to suitable for the portable application.

4.Water and ice can be replaced electrical fan to improve heat releasing of the portable device to obtain more temperature difference that can produce more electrical energy.

5. The thickness of CPCM should be decreased to increase heat from conductivity of CPCM that can be increased the total heat from portable device.

References

[1] S. P. Beeby, Z. Cao, and A. Almussallam, “Kinetic, thermoelectric and solar energy harvesting technologies for smart textiles,” *Multidiscip. Know-How Smart-Textiles Dev.*, pp. 306–328, 2013.

[2] N. Dang, E. Bozorgzadeh, and N. Venkatasubramanian, *Energy Harvesting for Sustainable Smart Spaces*, vol. 87. Elsevier Inc., 2012.

[3] S. Wu, D. Zhu, X. Zhang, and J. Huang, “Preparation and melting/freezing characteristics of Cu/paraffin nanofluid as phase-change material (PCM),” *Energy and Fuels*, vol. 24, no. 3, pp. 1894–1898, 2010.

[4] T. Qian, J. Li, X. Min, W. Guan, Y. Deng, and L. Ning, “Enhanced thermal conductivity of PEG/diatomite shape-stabilized phase change materials with Ag nanoparticles for thermal energy storage,” *J. Mater. Chem. A*, vol. 3, no. 16, pp. 8526–8536, 2015.

[5] C. Y. Zhao, W. Lu, and Y. Tian, “Heat transfer enhancement for thermal energy storage using metal foams embedded within phase change materials (PCMs),” *Sol. Energy*, vol. 84, no. 8, pp. 1402–1412, 2010.

[6] X. Xiao, P. Zhang, and M. Li, “Preparation and thermal characterization of paraffin/metal foam composite phase change material,” *Appl. Energy*, vol. 112, pp. 1357–1366, 2013.

[7] W. Wang, X. Yang, Y. Fang, J. Ding, and J. Yan, “Preparation and thermal properties of polyethylene glycol/expanded graphite blends for energy storage,” *Appl. Energy*, vol. 86, no. 9, pp. 1479–1483, 2009.

[8] Y. Cui, C. Liu, S. Hu, and X. Yu, “The experimental exploration of carbon nanofiber and carbon nanotube additives on thermal behavior of phase change materials,” *Sol. Energy Mater. Sol. Cells*, vol. 95, no. 4, pp. 1208–1212, 2011.

[9] A. Mikhalchan *et al.*, “Continuous and scalable fabrication and multifunctional properties of carbon nanotube aerogels from the floating catalyst method,” *Carbon N. Y.*, 2016.

[10] D. Medved, M. Kvakovský, and V. Sklenárová, “Intensive Programme " Renewable Energy Sources " LATENT HEAT STORAGE SYSTEMS,” vol. i, no. May, 2010.

[11] M. Mofijur *et al.*, “Phase change materials (PCM) for solar energy usages and storage,” *Energies*, vol. 12, no. 16, pp. 1–20, 2019.

[12] M. Torabi *et al.*, “We are IntechOpen , the world ’ s leading publisher of Open Access books Built by scientists , for scientists TOP 1 %,” *Intech*, vol. i, no. tourism, p. 13, 2016.

[13] M. A. Nessim and S. A. Elariane, “Review on Phase Change Materials and Its Applications in Buildings: Case Study of Egypt,” *SSRN Electron. J.*, no. 1, 2018.

[14] P. C. Materials, R. H. Energy, and S. Dryer, “วัสดุเปลี่ยนเฟสเพื่อช่วยรักษาความร้อนในเครื่องอบพลังงานแสงอาทิตย์ Phase Change Materials for Retaining Heat Energy in Solar Dryer,” pp. 258–261.

[15] A. M. Abdulateef, S. Mat, J. Abdulateef, K. Sopian, and A. A. Al-Abidi, “Geometric and design parameters of fins employed for enhancing thermal energy storage systems: a review,” *Renew. Sustain. Energy Rev.*, vol. 82, no. June, pp. 1620–1635, 2018.

[16] S. Krist and S. Krist, “Carnauba Wax,” *Veg. Fats Oils*, vol. 6, pp. 179–183, 2020.

[17] L. S. K. Dassanayake, D. R. Kodali, S. Ueno, and K. Sato, “Physical properties of rice bran wax in bulk and organogels,” *JAOCS, J. Am. Oil Chem. Soc.*, vol. 86, no. 12, pp. 1163–1173, 2009.

[18] N. Syahida, I. Fitry, A. Zuriyati, and N. Hanani, “Effects of palm wax on the physical, mechanical and water barrier properties of fish gelatin films for food packaging application,” *Food Packag. Shelf Life*, vol. 23, no. November 2019, p. 100437, 2020.

[19] S. Charumanee, S. Yotsawimonwat, P. Sirisa-ard, and K. Pholsongkram, “Characterization and chemical composition of epicuticular wax from banana leaves grown in Northern Thailand,” vol. 39, no. 4, pp. 509–516, 2017.

[20] N. M. S. Hidayah *et al.*, “Comparison on graphite, graphene oxide and reduced graphene oxide: Synthesis and characterization,” *AIP Conf. Proc.*, vol. 1892, 2017.

[21] N. I. Zaaba, K. L. Foo, U. Hashim, S. J. Tan, W. W. Liu, and C. H. Voon, “Synthesis of Graphene Oxide using Modified Hummers Method: Solvent Influence,” *Procedia Eng.*, vol. 184, pp. 469–477, 2017.

[22] H. K. Chae *et al.*, “A route to high surface area, porosity and inclusion of large molecules in crystals,” *Nature*, vol. 427, no. 6974, pp. 523–527, 2004.

[23] A. A. Balandin *et al.*, “Superior thermal conductivity of single-layer graphene,” *Nano Lett.*, vol. 8, no. 3, pp. 902–907, 2008.

[24] S. Chen *et al.*, “Thermal conductivity of isotopically modified graphene,” *Nat. Mater.*, vol. 11, no. 3, pp. 203–207, 2012.

[25] F. Liu, P. Ming, and J. Li, “Ab initio calculation of ideal strength and phonon instability of graphene under tension,” *Phys. Rev. B - Condens. Matter Mater. Phys.*, vol. 76, no. 6, pp. 1–7, 2007.

[26] C. Lee, X. Wei, J. W. Kysar, and J. Hone, “Measurement of the elastic properties and intrinsic strength of monolayer graphene,” *Science (80-.).*, vol. 321, no. 5887, pp. 385–388, 2008.

[27] M. J. Allen, V. C. Tung, and R. B. Kaner, “Honeycomb carbon: A review of graphene,” *Chem. Rev.*, vol. 110, no. 1, pp. 132–145, 2010.

[28] O. C. Compton and S. T. Nguyen, “Graphene oxide, highly reduced graphene oxide, and graphene: Versatile building blocks for carbon-based materials,” *Small*, vol. 6, no. 6, pp. 711–723, 2010.

[29] D. R. Dreyer, S. Park, C. W. Bielawski, and R. S. Ruoff, “The chemistry of graphene oxide,” *Chem. Soc. Rev.*, vol. 39, no. 1, pp. 228–240, 2010.

[30] L. Liu, K. Zheng, Y. Yan, Z. Cai, S. Lin, and X. Hu, “Graphene Aerogels Enhanced Phase Change Materials prepared by one-pot method with high thermal conductivity and large latent energy storage,” *Solar Energy Materials and Solar Cells*, vol. 185. pp. 487–493, 2018.

[31] W. Park, J. Hu, L. A. Jauregui, X. Ruan, and Y. P. Chen, “Electrical and thermal conductivities of reduced graphene oxide/polystyrene composites. (arXiv:1403.2467v2 [cond-mat.mtrl-sci] UPDATED),” pp. 1–13.

[32] S. Harish, D. Orejon, Y. Takata, and M. Kohno, “Thermal conductivity enhancement of lauric acid phase change nanocomposite with graphene nanoplatelets,” *Appl. Therm. Eng.*, vol. 80, pp. 205–211, 2015.

[33] C. Phrompet, C. Sriwong, and C. Ruttanapun, “Mechanical, dielectric, thermal and antibacterial properties of reduced graphene oxide (rGO)-nanosized C3AH6 cement nanocomposites for smart cement-based materials,” *Compos. Part B Eng.*, vol. 175, no. June, p. 107128, 2019.

[34] R. J. Warzoha, R. M. Weigand, and A. S. Fleischer, “Temperature-dependent thermal properties of a paraffin phase change material embedded with herringbone style graphite nanofibers,” *Appl. Energy*, vol. 137, pp. 716–725, 2015.

[35] J. Sarkar and S. Bhattacharyya, “Application of graphene and graphene-based materials in clean energy-related devices Minghui,” *Arch. Thermodyn.*, vol. 33, no. 4, pp. 23–40, 2012.

[36] W. Li, Y. Dong, X. Zhang, and X. Liu, “Preparation and Performance Analysis of Graphite Additive/Paraffin Composite Phase Change Materials,” *Processes*, vol. 7, no. 7, p. 447, 2019.

[37] X. Zhao, “Investigation of a novel phase change composite material for condensation heat recovery in cold storages,” pp. 2–19, 2017.

[38] M. Nourani, N. Hamdami, J. Keramat, A. Moheb, and M. Shahedi, “Thermal behavior of paraffin-nano-Al2O3 stabilized by sodium stearoyl lactylate as a stable phase change material with high thermal conductivity,” *Renew. Energy*, vol. 88, pp. 474–482, 2016.

[39] Y. Yang, J. Luo, G. Song, Y. Liu, and G. Tang, “Thermochimica Acta The experimental exploration of nano-Si 3 N 4 / paraf fi n on thermal behavior of phase change materials,” *Thermochim. Acta*, vol. 597, pp. 101–106, 2014.

[40] M. N. Mohd Iqbaldin, I. Khudzir, M. I. Mohd Azlan, A. G. Zaidi, B. Surani, and Z. Zubri, “Properties of coconut shell activated carbon,” *J. Trop. For. Sci.*, vol. 25, no. 4, pp. 497–503, 2013.

[41] Z. Jin, B. Tian, L. Wang, and R. Wang, “Comparison on thermal conductivity and permeability of granular and consolidated activated carbon for refrigeration,” *Chinese J. Chem. Eng.*, vol. 21, no. 6, pp. 676–682, 2013.

[42] T. Khadiran, M. Z. Hussein, Z. Zainal, and R. Rusli, “Shape-stabilised n-octadecane/activated carbon nanocomposite phase change material for thermal energy storage,” *J. Taiwan Inst. Chem. Eng.*, vol. 55, pp. 189–197, 2015.

[43] A. Ertas, C. T. R. Boyce, and U. Gulbulak, “Experimental measurement of bulk thermal conductivity of activated carbon with adsorbed natural gas for Ang energy storage tank design application,” *Energies*, vol. 13, no. 3, 2020.

[44] L. Jiang, R. Z. Wang, and A. P. Roskilly, “Development and thermal characteristics of a novel composite oleic acid for cold storage,” *Int. J. Refrig.*, vol. 100, pp. 55–62, 2019.

[45] S. M. Santhi Rekha and S. Sukchai, “Design of phase change material based domestic solar cooking system for both indoor and outdoor cooking applications,” *J. Sol. Energy Eng. Trans. ASME*, vol. 140, no. 4, pp. 1–8, 2018.

[46] A. Kumar, G. Kumar, and S. A. I. Nath, “DESIGN AND FABRICATION OF HOT WATER TANK USING PHASE CHANGE MATERIAL WITH ANSYS MODEL,” vol. 14, no. 4, pp. 3037–3045, 2016.

[47] J. Fořt, A. Trník, M. Pavlíková, and Z. Pavlík, “Diatomite/Palm Wax Composite as a Phase Change Material for Latent Heat Storage,” *Adv. Mater. Res.*, vol. 1126, pp. 33–38, 2015.

[48] M. Helm, K. Hagel, W. Pfeffer, S. Hiebler, and C. Schweigler, “Solar heating and cooling system with absorption chiller and latent heat storage - A research project summary,” *Energy Procedia*, vol. 48, pp. 837–849, 2014.

[49] M. Helm, C. Keil, S. Hiebler, H. Mehling, and C. Schweigler, “Solar heating and cooling system with absorption chiller and low temperature latent heat storage: Energetic performance and operational experience,” *Int. J. Refrig.*, vol. 32, no. 4, pp. 596–606, 2009.

[50] M. Rouse, “What is Seebeck effect? - Definition from WhatIs.com.” 2008.

[51] U. Datta, S. Dessouky, and A. T. Papagiannakis, “Harvesting thermoelectric energy from asphalt pavements,” *Transp. Res. Rec.*, vol. 2628, no. November 2016, pp. 12–22, 2017.

[52] R. El-Araby, A. Amin, A. K. El Morsi, N. N. El-Ibiari, and G. I. El-Diwani, “Study on the characteristics of palm oil–biodiesel–diesel fuel blend,” *Egypt. J. Pet.*, vol. 27, no. 2, pp. 187–194, 2018.

[53] “Phase Change with Convection: Modelling and Validation,” *Phase Change with Convection: Modelling and Validation*. 2004.

APPENDIX

Appendix A: Properties of material

Appendix B: Experimental result and calculation

Appendix B-1: Experimental result of selection of suitable PCM

Appendix B-2: Experimental result of thermal property enhancement of PCM

Appendix B-3: Calculation of power of portable device

Appendix B-4 Experimental result of experimental setup of prototype of a portable device

Appendix A: Properties of material

Table A-1 : Properties of CPCMs

CPCM	Melting point (°C)	Thermal diffusivity (mm^2/s)	Specific heat capacity (MJ/m^3K)
Pure palm wax	40.3 ± 0.339	0.134 ± 0.002	1.545 ± 0.020
0.5% AC	40.2 ± 0.113	0.117 ± 0.002	1.856 ± 0.025
1.0% AC	40.0 ± 0.226	0.106 ± 0.004	2.180 ± 0.048
1.5% AC	40.1 ± 0.078	0.105 ± 0.002	2.181 ± 0.022
2.0% AC	40.3 ± 0.057	0.115 ± 0.001	2.026 ± 0.008
2.5% AC	40.0 ± 0.042	0.149 ± 0.004	1.601 ± 0.030

Appendix B: Experimental result and calculation

Appendix B-1: Experimental results of selection of suitable PCM

Table B-1-1 Data of charging and discharging cycle of paraffin wax and palm wax

Time (min)	Temperature (ºC)							
	Paraffin wax				Palm wax			
	1st	2nd	AVG	STD	1st	2nd	AVG	STD
0	28.9	28.9	28.9	0.000	29.4	29.4	29.4	0.000
1	40.0	38.5	39.3	1.061	36.1	36.2	36.2	0.071
2	48.1	47.9	48.0	0.141	41.6	43.8	42.7	1.556
3	52.9	52.3	52.6	0.448	48.6	50.2	49.4	1.131
4	75.9	75.7	75.8	0.106	56.4	57.0	56.7	0.424
5	79.4	80.2	79.8	0.566	79.7	81.5	80.6	1.273
6	84.2	83.5	83.9	0.495	82.7	85.7	84.2	2.121
7	86.0	85.0	85.5	0.707	84.8	86.2	85.5	0.990
8	86.2	85.7	86.0	0.354	85.4	86.4	85.9	0.707
9	86.3	86.2	86.3	0.071	85.8	86.6	86.2	0.566
10	86.4	86.3	86.4	0.071	86.1	86.7	86.4	0.424
11	86.5	86.3	86.4	0.141	86.3	86.7	86.5	0.283
12	86.5	86.4	86.5	0.071	86.5	86.7	86.6	0.141
13	86.6	86.4	86.5	0.141	86.6	86.8	86.7	0.141
14	86.5	86.5	86.5	0.000	86.6	86.8	86.7	0.141
15	86.5	86.5	86.5	0.000	86.7	86.7	86.7	0.000
16	86.5	86.5	86.5	0.000	86.7	86.7	86.7	0.000
17	86.6	86.5	86.6	0.071	86.7	86.7	86.7	0.000
18	86.6	86.6	86.6	0.000	86.7	86.7	86.7	0.000
19	86.6	86.6	86.6	0.000	86.7	86.7	86.7	0.000
20	86.6	86.6	86.6	0.000	86.7	86.7	86.7	0.000
21	86.6	86.6	86.6	0.000	58.5	60.5	59.5	1.414
22	86.6	86.6	86.6	0.000	47.9	48.1	48.0	0.141
23	86.6	86.6	86.6	0.000	43.2	43.8	43.5	0.424
24	85.7	85.2	85.5	0.354	39.3	42.4	40.9	2.192
25	59.4	62.4	60.9	2.121	38.7	42.5	40.6	2.687
26	57.8	55.8	56.8	1.414	37.0	41.2	39.1	2.970
27	56.9	51.4	54.2	3.889	35.2	39.0	37.1	2.687
28	53.3	52.8	53.1	0.354	32.3	37.3	34.8	3.536
29	44.2	39.0	41.6	3.677	31.4	36.1	33.8	3.323
30	38.4	35.2	36.8	2.263	30.5	35.2	32.9	3.323
31	34.5	32.5	33.5	1.414	30.3	33.9	32.1	2.546
32	31.6	30.7	31.2	0.636	29.7	32.1	30.9	1.697
33	29.9	29.7	29.8	0.141	28.8	30.1	29.5	0.919
34	29.1	29.2	29.2	0.071	28.6	29.7	29.2	0.778

Table B-1-1 Data of charging and discharging cycle of paraffin wax and palm wax (Cont.)

Time (min)	Temperature (ºC)							
	Paraffin wax				Palm wax			
	1st	2nd	AVG	STD	1st	2nd	AVG	STD
34	29.1	29.2	29.2	0.071	28.6	29.7	29.2	0.778
35	28.0	28.8	28.4	0.566	28.2	29.3	28.8	0.778
36	27.7	28.6	28.2	0.636	28.0	29.2	28.6	0.849
37	27.6	28.5	28.1	0.636	27.7	29.1	28.4	0.990
38	27.5	28.5	28.0	0.707	27.5	29.0	28.3	1.061
39	27.5	28.4	28.0	0.636	27.3	28.9	28.1	1.131
40	27.5	28.4	28.0	0.636	27.3	28.9	28.1	1.131
41	27.4	28.4	27.9	0.707	27.2	28.9	28.1	1.202
42	27.4	28.4	27.9	0.707	27.2	28.8	28.0	1.131
43	27.4	28.3	27.9	0.636	27.2	28.8	28.0	1.131
44	27.3	28.3	27.8	0.707	27.1	28.8	28.0	1.202
45	27.3	28.3	27.8	0.707	27.1	28.8	28.0	1.202
46	27.3	28.3	27.8	0.707	27.1	28.7	27.9	1.131
47	27.3	28.3	27.8	0.707	27.1	28.7	27.9	1.131
48	27.3	28.3	27.8	0.707	27.1	28.7	27.9	1.131
49					27.1	28.7	27.9	1.131
50					27.1	28.7	27.9	1.131

Table B-1-2 Data of charging and discharging cycle of carnauba wax and rice bran wax

Time (min)	Temperature (ºC)							
	Carnauba wax				Rice bran wax			
	1st	2nd	AVG	STD	1st	2nd	AVG	STD
0	29.4	29.3	29.4	0.071	29.0	28.8	28.9	0.141
1	40.5	41.7	41.1	0.849	41.9	43.7	42.8	1.273
2	55.7	57.9	56.8	1.556	55.1	54.7	54.9	0.283
3	67.9	65.7	66.8	1.556	62.9	63.4	63.2	0.354
4	70.3	72.9	71.6	1.838	67.2	69.6	68.4	1.697
5	71.9	73.1	72.5	0.849	69.7	71.8	70.8	1.485
6	73.0	73.9	73.5	0.636	71.3	73.1	72.2	1.273
7	74.2	74.8	74.5	0.424	73.1	74.1	73.6	0.707
8	75.2	75.7	75.5	0.354	74.2	75.0	74.6	0.566
9	76.0	76.6	76.3	0.424	74.8	76.0	75.4	0.849
10	76.9	77.4	77.2	0.354	75.3	77.5	76.4	1.556
11	77.8	78.2	78.0	0.283	76.4	81.8	79.1	3.818
12	80.0	79.0	79.5	0.707	81.4	84.4	82.9	2.121
13	80.2	80.1	80.2	0.071	84.0	85.6	84.8	1.131

Table B-1-2 Data of charging and discharging cycle of carnauba wax and rice bran wax (Cont.)

Time (min)	Temperature (ºC)							
	Carnauba wax				Rice bran wax			
	1st	2nd	AVG	STD	1st	2nd	AVG	STD
14	81.9	81.4	81.7	0.354	85.7	86.1	85.9	0.283
15	84.1	83.8	84.0	0.212	86.2	86.5	86.4	0.212
16	85.5	85.1	85.3	0.283	86.4	86.6	86.5	0.141
17	85.7	85.9	85.8	0.141	86.6	86.6	86.6	0.000
18	85.7	86.3	86.0	0.424	86.6	86.6	86.6	0.000
19	85.8	86.7	86.3	0.636	86.7	86.7	86.7	0.000
20	85.9	86.8	86.4	0.636	86.7	86.7	86.7	0.000
21	85.9	86.9	86.4	0.707	86.8	86.8	86.8	0.000
22	85.9	87.0	86.5	0.778	86.9	86.7	86.8	0.141
23	86.6	87.1	86.9	0.354	86.9	86.8	86.9	0.071
24	86.6	87.1	86.9	0.354	87.0	86.8	86.9	0.141
25	86.6	87.1	86.9	0.354	87.0	86.7	86.9	0.212
26	86.6	87.2	86.9	0.424	87.1	86.8	87.0	0.212
27	86.6	87.2	86.9	0.424	87.1	86.8	87.0	0.212
28	86.6	87.2	86.9	0.424	87.1	86.8	87.0	0.212
29	86.6	87.2	86.9	0.424	87.1	86.8	87.0	0.212
30	86.6	87.2	86.9	0.424	87.1	86.8	87.0	0.212
31	86.6	87.2	86.9	0.424	87.1	86.8	87.0	0.212
32	82.5	81.2	81.9	0.919	87.1	86.9	87.0	0.141
33	78.3	76.7	77.5	1.131	87.1	86.9	87.0	0.141
34	66.2	65.7	66.0	0.354	87.1	86.9	87.0	0.141
35	46.2	47.7	47.0	1.061	87.1	86.9	87.0	0.141
36	43.6	40.1	41.9	2.475	87.1	86.9	87.0	0.141
37	34.0	32.3	33.2	1.202	87.1	86.9	87.0	0.141
38	29.9	30.1	30.0	0.141	83.1	80.3	81.7	1.980
39	29.3	29.5	29.4	0.141	77.6	73.8	75.7	2.687
40	28.8	29.3	29.1	0.354	71.4	67.0	69.2	3.111
41	28.4	29.0	28.7	0.424	62.5	58.1	60.3	3.111
42	28.1	28.9	28.5	0.566	49.9	48.9	49.4	0.707
43	27.9	28.9	28.4	0.707	43.2	42.0	42.6	0.849
44	27.7	28.9	28.3	0.849	37.0	36.1	36.6	0.636
45	27.7	28.8	28.3	0.778	36.1	35.1	35.6	0.707
46	27.6	28.8	28.2	0.849	28.9	29.2	29.1	0.212
47	27.6	28.8	28.2	0.849	28.9	29.0	29.0	0.071
48	27.6	28.8	28.2	0.849	28.8	28.9	28.9	0.071
49	27.5	28.8	28.2	0.919	28.7	28.9	28.8	0.141
50	27.5	28.8	28.2	0.919	28.6	28.9	28.8	0.212

Table B-1-2 Data of charging and discharging cycle of carnauba wax and rice bran wax (Cont.)

Time (min)	Temperature (ºC)							
	Carnauba wax				Rice bran wax			
	1st	2nd	1st	2nd	1st	2nd	1st	2nd
51	27.5	28.8	28.2	0.919	28.6	28.8	28.7	0.141
52	27.5	28.8	28.2	0.919	28.6	28.7	28.7	0.071
53	27.5	28.8	28.2	0.919	28.4	28.7	28.6	0.212
54					28.1	28.6	28.4	0.354
55					28.1	28.5	28.3	0.283

Appendix B-2: Experimental result of thermal property enhancement of PCM

Table B-2-1 Result of carbon (C) and oxygen (O) percentage by weight in CPCMs from TAC analysis

Percentage by weight (%)	1st				2nd			
	Weight (%)		Atomic (%)		Weight (%)		Atomic (%)	
	C	O	C	O	C	O	C	O
Pure palm	85.79	14.21	88.94	11.06	84.84	15.16	88.17	11.83
0.5 AC	85.44	14.56	88.66	11.34	84.97	15.03	88.28	11.72
1.0AC	85.84	14.16	88.98	11.02	85.09	14.91	88.37	11.63
1.5AC	85.98	14.02	89.09	10.91	85.37	14.63	88.6	11.4
2.0AC	86.06	13.94	89.15	10.85	86.16	13.84	89.24	10.76
2.5AC	86.45	13.55	89.47	10.53	86.83	13.17	89.78	10.22

Table B-2-2 Data of charging and discharging cycle of pure palm wax

Time (min)	Temperature (ºC)						AVG	STD
	Pure palm wax (1)			Pure palm wax (2)				
	1st	2nd	3rd	1st	2nd	3rd		
0	31.9	31.9	31.9	**31.9**	**31.9**	31.9	31.9	0.000
1	39.7	39.5	39.2	38.9	39.2	38.8	39.0	0.208
2	47.4	47.1	46.9	46.4	46.7	46.5	46.5	0.153
3	52.0	51.9	51.8	51.2	51.3	51.2	51.2	0.058
4	61.2	61.1	60.7	60.4	60.6	60.3	60.4	0.153
5	71.5	71.6	71.4	71.3	71.4	71.2	71.3	0.100
6	74.0	74.0	73.9	73.8	74.0	73.7	73.8	0.153
7	74.9	74.9	74.6	74.7	74.8	74.5	74.7	0.153
8	75.2	75.1	75.0	75.0	75.2	74.9	75.0	0.153

Table B-2-2 Data of charging and discharging cycle of pure palm wax (Cont.)

Time (min)	Temperature (ºC)						AVG	STD
	Pure palm wax (1)			Pure palm wax (2)				
	1st	2nd	3rd	1st	2nd	3rd		
9	75.4	75.4	75.1	75.2	75.3	75.0	75.2	0.014
10	75.5	75.8	75.3	75.2	75.3	75.1	75.4	0.107
11	75.5	75.8	75.3	75.3	75.4	75.1	75.4	0.070
12	75.5	75.9	75.4	75.3	75.4	75.3	75.5	0.146
13	75.6	76.0	75.6	75.5	75.5	75.3	75.6	0.082
14	75.6	76.0	75.6	75.5	75.5	75.4	75.6	0.122
15	75.7	76.1	75.6	75.6	75.5	75.4	75.7	0.116
16	75.7	76.1	75.7	75.6	75.6	75.5	75.7	0.122
17	75.8	76.1	75.7	75.6	75.7	75.6	75.8	0.106
18	75.8	76.2	75.8	75.6	75.7	75.7	75.8	0.122
19	75.8	76.2	75.8	75.7	75.8	75.7	75.8	0.122
20	75.9	76.2	75.8	75.7	75.8	75.7	75.9	0.106
21	61.8	61.4	61.9	60.1	60.0	59.7	60.8	0.040
22	49.7	49.4	49.8	48.0	47.8	47.6	48.7	0.006
23	43.7	43.5	43.9	43.6	43.6	43.3	43.6	0.019
24	42.0	41.8	42.3	42.1	42.0	41.7	42.0	0.031
25	41.9	41.7	42.1	41.8	41.7	41.5	41.8	0.033
26	41.6	41.5	41.7	41.6	41.5	41.3	41.5	0.037
27	40.6	40.5	40.8	40.7	40.7	40.5	40.6	0.026
28	39.5	39.4	39.7	39.5	39.3	39.2	39.4	0.000
29	38.0	37.9	38.2	37.8	37.6	37.7	37.9	0.037
30	36.5	36.3	36.7	36.4	36.3	36.3	36.4	0.101
31	34.9	34.7	35.1	34.7	34.5	34.3	34.7	0.000
32	33.8	33.7	33.9	33.3	33.2	33.0	33.5	0.037
33	32.8	32.6	32.9	32.4	33.1	32.1	32.7	0.255
34	32.1	32.0	32.3	31.8	31.6	31.5	31.9	0.000
35	31.6	31.3	31.8	31.4	31.2	31.1	31.4	0.070
36	31.0	30.9	31.4	31.0	30.9	30.8	31.0	0.116
37	30.9	30.8	31.1	30.9	30.8	30.7	30.9	0.037
38	30.8	30.8	31.0	30.8	30.8	30.7	30.8	0.041
39	30.8	30.7	30.9	30.8	30.8	30.7	30.8	0.030
40	30.8	30.7	30.9	30.8	30.7	30.6	30.8	0.000
41	30.7	30.7	30.8	30.8	30.7	30.6	30.7	0.030
42	30.7	30.7	30.7	30.7	30.7	30.6	30.7	0.041
43	30.7	30.6	30.6	30.7	30.7	30.6	30.7	0.000
44	30.6	30.6	30.5	30.6	30.6	30.5	30.6	0.000
45	30.6	30.5	30.5	30.5	30.6	30.5	30.5	0.000
46	30.6	30.5	30.5	30.5	30.6	30.5	30.5	0.000

Table B-2-2 Data of charging and discharging cycle of pure palm wax (Cont.)

Time (min)	Temperature (ºC)							
	Pure palm wax (1)			Pure palm wax (2)			AVG	STD
	1st	2nd	3rd	1st	2nd	3rd		
47	30.6	30.5	30.5	30.5	30.6	30.5	30.5	0.000
48	30.6	30.5	30.5	30.5	30.6	30.4	30.5	0.030
49	30.5	30.5	30.4	30.5	30.5	30.4	30.5	0.000
50	30.5	30.5	30.4	30.5	30.5	30.4	30.5	0.000

Table B-2-3 Data of charging and discharging cycle of 0.5 wt% AC

Time (min)	Temperature (◦C)							
	0.5 wt% AC (1)			0.5 wt% AC (2)			AVG	STD
	1st	2nd	3rd	1st	2nd	3rd		
0	31.9	31.9	31.9	31.9	31.9	31.9	31.9	0.000
1	39.6	39.2	39.7	39.8	39.3	39.4	39.5	0.000
2	48.5	48.3	48.8	48.3	48.1	48.2	48.4	0.107
3	54.3	54	54.5	53	52.8	53	53.6	0.096
4	65.4	64.9	65.6	64.7	64.3	64.5	64.9	0.114
5	70.7	70.3	70.8	70.7	70.4	70.2	70.5	0.009
6	72.4	72.2	73	72.4	72.4	72.1	72.4	0.172
7	73.1	73	73.8	73.4	73.2	73	73.3	0.167
8	73.6	73.5	74	73.8	73.4	73.5	73.6	0.040
9	74	73.8	74.2	74.1	73.9	74	74.0	0.071
10	74.2	74	74.4	74.4	74.1	74.3	74.2	0.033
11	74.6	74.2	74.7	74.6	74.4	74.5	74.5	0.116
12	75	74.4	75	74.8	74.6	74.9	74.8	0.137
13	75	74.5	75.1	75.1	74.9	75.2	75.0	0.119
14	75.3	75.1	75.4	75.3	75	75.4	75.3	0.039
15	75.3	75.2	75.4	75.3	75.3	75.5	75.3	0.011
16	75.4	75.3	75.5	75.4	75.4	75.5	75.4	0.030
17	75.5	75.4	75.6	75.6	75.5	75.7	75.6	0.000
18	75.6	75.4	75.7	75.6	75.5	75.8	75.6	0.000
19	75.7	75.5	75.7	75.7	75.6	75.9	75.7	0.026
20	75.7	75.5	75.8	75.7	75.6	75.9	75.7	0.000
21	59.3	59.1	59.4	59.9	60	60.1	59.6	0.037
22	47.8	47.6	48	48.6	48.4	48.9	48.2	0.037
23	43.6	43.3	43.6	43.7	43.5	43.9	43.6	0.019
24	41.5	41.4	41.6	41.6	41.5	42	41.6	0.116
25	41.4	41.2	41.5	41.5	41.3	41.7	41.4	0.033
26	40.5	40.2	40.6	40.9	40.6	41.1	40.7	0.031

Table B-2-3 Data of charging and discharging cycle of 0.5 wt% AC (Cont.)

Time (min)	Temperature (◦C)							
	0.5 wt% AC (1)			0.5 wt% AC (2)			AVG	STD
	1st	2nd	3rd	1st	2nd	3rd		
27	39.4	39.3	39.8	40	39.9	40.4	39.8	0.000
28	37.9	37.8	38.2	38.5	38.7	38.9	38.3	0.006
29	36.0	35.9	36.4	36.6	36.4	36.9	36.4	0.009
30	34.7	34.6	35.0	35.2	35.0	35.5	35.0	0.031
31	33.3	33.1	33.5	33.5	33.6	33.8	33.5	0.033
32	32.3	32.0	32.6	32.6	32.5	33	32.5	0.025
33	31.8	31.5	32.1	32.3	32.3	32.4	32.1	0.171
34	31.4	31.2	31.7	31.5	31.1	31.7	31.4	0.038
35	31.1	30.9	31.4	31.1	31.0	31.5	31.2	0.009
36	31.0	30.8	31.2	31.2	30.9	31.4	31.1	0.037
37	30.7	30.6	31.0	30.9	30.8	31.3	30.9	0.040
38	30.6	30.6	30.9	30.8	30.7	31.2	30.8	0.065
39	30.6	30.6	30.9	30.8	30.7	31.2	30.8	0.065
40	30.6	30.6	30.9	30.8	30.7	31.1	30.8	0.025
41	30.5	30.5	30.8	30.7	30.6	31.1	30.7	0.065
42	30.5	30.5	30.8	30.7	30.6	31.1	30.7	0.065
43	30.5	30.5	30.8	30.7	30.6	31.0	30.7	0.025
44	30.5	30.4	30.7	30.6	30.6	30.9	30.6	0.014
45	30.5	30.4	30.8	30.6	30.5	30.9	30.6	0.000
46	30.5	30.4	30.8	30.6	30.5	30.9	30.6	0.000
47	30.5	30.4	30.8	30.6	30.5	30.8	30.6	0.039
48	30.5	30.4	30.8	77.1	77.0	77.3	77.1	0.010
49	30.5	30.4	30.7	77.2	77.1	77.4	77.2	0.010
50	30.5	30.4	30.7	77.2	77.1	77.4	77.2	0.010

Table B-2-4 Data of charging and discharging cycle of 1.0 wt% AC

Time (min)	Temperature (°C)							
	1.0 wt% AC (1)			1.0 wt% AC (2)			AVG	STD
	1st	2nd	3rd	1st	2nd	3rd		
0	31.9	31.9	31.9	31.9	31.9	31.9	31.9	0.000
1	40.2	40.6	40.4	40.3	40.9	41.0	40.6	0.126
2	47.8	48.1	47.8	47.7	47.9	48.1	47.9	0.019
3	53.6	54.0	53.8	53.0	53.4	53.5	53.6	0.046
4	66.6	66.9	66.8	63.7	64.0	64.3	65.4	0.104
5	72.0	72.4	72.2	71.6	71.8	72.1	72.0	0.037
6	73.3	73.8	73.5	72.9	73.1	73.3	73.3	0.037
7	74.6	74.9	74.8	74.6	74.7	74.9	74.8	0.000

Table B-2-4 Data of charging and discharging cycle of 1.0 wt% AC (Cont.)

Time (min)	Temperature (◦C)							
	0.5 wt% AC (1)			0.5 wt% AC (1)			AVG	STD
	1st	2nd	3rd	1st	2nd	3rd		
8	74.9	75.4	75.1	74.9	75.1	75.4	75.1	0.000
9	75.3	75.7	75.4	75.2	75.4	75.7	75.5	0.031
10	75.4	75.9	75.5	75.6	75.8	76.0	75.7	0.046
11	75.5	76.0	75.7	75.7	75.8	76.1	75.8	0.031
12	75.5	76.1	75.8	75.8	75.9	76.3	75.9	0.025
13	75.6	76.2	75.9	75.9	76.0	76.4	76.0	0.025
14	75.8	76.3	76.0	76.0	76.0	76.4	76.1	0.015
15	75.9	76.4	76.0	76.1	76.1	76.5	76.2	0.024
16	75.9	76.4	76.0	76.1	76.2	76.5	76.2	0.040
17	76.1	76.5	76.1	76.1	76.2	76.6	76.3	0.024
18	76.1	76.6	76.1	76.2	76.2	76.6	76.3	0.041
19	76.2	76.7	76.2	76.2	76.3	76.6	76.4	0.057
20	76.2	76.7	76.2	76.2	76.3	76.6	76.4	0.057
21	59.3	59.7	59.4	59.1	59.2	59.4	59.4	0.039
22	47.3	47.8	47.5	46.6	46.7	47.0	47.2	0.031
23	42.8	43.1	42.8	42.4	42.6	42.7	42.7	0.014
24	41.6	41.7	41.4	40.8	41.0	41.4	41.3	0.108
25	40.8	41.0	40.6	40.4	40.6	40.8	40.7	0.000
26	40.1	40.3	39.9	39.5	39.7	39.9	39.9	0.000
27	38.8	39.0	38.7	38.2	38.4	38.5	38.6	0.000
28	37.9	38.1	37.7	37.2	37.4	37.7	37.7	0.037
29	35.6	35.9	35.5	35.2	35.3	35.7	35.5	0.040
30	35.2	35.0	35.1	34.3	34.0	34.5	34.7	0.107
31	33.7	33.9	33.5	33.0	33.2	33.5	33.5	0.037
32	32.4	32.7	32.3	32.1	32.4	32.7	32.4	0.065
33	31.7	32.2	31.9	31.3	31.4	31.8	31.7	0.009
34	31.5	31.8	31.4	31.0	31.1	31.4	31.4	0.000
35	31.2	31.4	31.1	30.6	30.9	31.2	31.1	0.104
36	31.0	31.2	30.7	30.5	30.6	30.8	30.8	0.070
37	30.9	31.0	30.7	30.5	30.6	30.7	30.7	0.037
38	30.8	30.9	30.6	30.5	30.5	30.7	30.7	0.026
39	30.7	30.8	30.6	30.5	30.4	30.6	30.6	0.000
40	30.7	30.8	30.6	30.5	30.4	30.6	30.6	0.000
41	30.7	30.7	30.6	30.4	30.4	30.5	30.6	0.000
42	30.7	30.7	30.5	30.4	30.4	30.5	30.5	0.041
43	30.6	30.7	30.5	30.4	30.4	30.5	30.5	0.030
44	30.6	30.6	30.5	30.4	30.3	30.5	30.5	0.030

Table B-2-4 Data of charging and discharging cycle of 1.0 wt% AC (Cont.)

Time (min)	Temperature (°C)						AVG	STD
	1.0 wt% AC (1)			1.0 wt% AC (2)				
	1st	2nd	3rd	1st	2nd	3rd		
45	30.5	30.6	30.5	30.4	30.3	30.4	30.5	0.000
46	30.5	30.6	30.4	30.3	30.3	30.4	30.4	0.030
47	30.5	30.5	30.4	30.3	30.3	30.4	30.4	0.000
48	30.4	30.5	30.4	30.3	30.3	30.3	30.4	0.041
49	30.4	30.5	30.4	30.3	30.3	30.3	30.4	0.041
50	30.4	30.5	30.4	30.3	30.3	30.3	30.4	0.041

Table B-2-5 Data of charging and discharging cycle of 1.5 wt% AC

Time (min)	Temperature (°C)						AVG	STD
	1.5 wt% AC (1)			1.5 wt% AC (2)				
	1st	2nd	3rd	1st	2nd	3rd		
0	31.9	31.9	31.9	31.9	31.9	31.9	31.9	0.000
1	42.4	42	42.1	41.6	41.8	41.4	41.9	0.006
2	50.7	50.5	50.6	49	49.6	49.3	50.0	0.141
3	56.2	55.8	56.1	55.5	55.8	55.4	55.8	0.000
4	70.0	69.5	69.8	69.3	69.9	69.1	69.6	0.116
5	73.6	73.2	73.4	72.3	72.5	72.1	72.9	0.000
6	74.3	73.8	74.2	74.1	74.2	73.9	74.1	0.079
7	75.0	74.5	74.7	74.7	74.9	74.5	74.7	0.037
8	75.5	75.1	75.2	75.3	75.4	75	75.3	0.000
9	75.8	75.3	75.5	75.5	75.7	75.4	75.5	0.070
10	75.9	75.4	75.6	75.5	76	75.3	75.6	0.077
11	76.2	75.8	76.0	75.8	76	75.6	75.9	0.000
12	76.3	75.9	76.1	75.9	76.1	75.7	76.0	0.000
13	76.4	76.1	76.2	76.0	76.1	75.7	76.1	0.039
14	76.4	76.2	76.3	76.0	76.3	75.9	76.2	0.076
15	76.4	76.3	76.3	76.0	76.3	75.9	76.2	0.106
16	76.4	76.3	76.3	76.1	76.4	76	76.3	0.106
17	76.5	76.1	76.2	76.2	76.4	76.1	76.3	0.039
18	76.5	76.1	76.2	76.2	76.4	76.1	76.3	0.039
19	76.5	76.2	76.3	76.3	76.4	76.1	76.3	0.000
20	76.5	76.2	76.3	76.3	76.4	76.1	76.3	0.000
21	59.1	59	58.8	58.6	58.9	58.4	58.8	0.070
22	45.9	46.0	46.1	45.3	45.5	45	45.6	0.107
23	41.9	42.0	42.2	41.4	41.6	41.3	41.7	0.000
24	40.9	41.1	41.3	40.4	40.5	40.2	40.7	0.033
25	40.4	40.5	40.7	40.1	40.3	39.9	40.3	0.033

Table B-2-5 Data of charging and discharging cycle of 1.5 wt% AC

Time (min)	Temperature (ºC)							
	1.0 wt% AC (1)			1.0 wt% AC (1)			AVG	STD
	1st	2nd	3rd	1st	2nd	3rd		
26	39.2	39.4	39.6	38.7	39.1	38.6	39.1	0.046
27	37.9	37.6	38	37.4	37.5	37.2	37.6	0.039
28	36.6	36.3	36.9	34.1	34.5	34.0	35.4	0.025
29	34.8	34.7	35.1	34.4	34.7	34.1	34.6	0.065
30	33.6	33.2	33.9	33.3	33.6	33.2	33.5	0.101
31	32.6	32.5	32.7	32	32.2	31.7	32.3	0.107
32	31.9	31.8	32.1	31.3	31.6	31	31.6	0.104
33	31.6	31.5	31.9	31.2	31.4	30.9	31.4	0.031
34	31.1	31.1	31.2	31.1	31.3	30.8	31.1	0.137
35	30.9	30.9	31.1	30.8	31.0	30.6	30.9	0.060
36	30.8	30.6	31.0	30.7	30.9	30.5	30.8	0.000
37	30.7	30.5	30.9	30.6	30.8	30.5	30.7	0.033
38	30.6	30.5	30.8	30.6	30.7	30.5	30.6	0.037
39	30.5	30.4	30.7	30.6	30.7	30.5	30.6	0.037
40	30.5	30.4	30.6	30.6	30.6	30.5	30.5	0.030
41	30.5	30.4	30.6	30.5	30.6	30.5	30.5	0.030
42	30.5	30.4	30.6	30.5	30.6	30.4	30.5	0.000
43	30.4	30.4	30.5	30.5	30.6	30.4	30.5	0.030
44	30.4	30.4	30.5	30.5	30.5	30.4	30.5	0.000
45	30.4	30.3	30.5	30.5	30.5	30.4	30.4	0.030
46	30.4	30.3	30.5	30.4	30.5	30.4	30.4	0.030
47	30.4	30.3	30.4	30.4	30.5	30.4	30.4	0.000
48	30.3	30.3	30.4	30.4	30.4	30.3	30.4	0.000
49	30.3	30.3	30.4	30.4	30.4	30.3	30.4	0.000
50	30.3	30.3	30.4	30.4	30.4	30.3	30.4	0.000

Table B-2-6 Data of charging and discharging cycle of 2.0 wt% AC

Time (min)	Temperature (ºC)							
	2.0 wt% AC (1)			2.0 wt% AC (2)			AVG	STD
	1st	2nd	3rd	1st	2nd	3rd		
0	31.9	31.9	31.9	31.9	31.9	31.9	31.9	0.000
1	42.5	42.6	42	43.3	43	42.9	42.7	0.080
2	50.4	50.6	50.3	51.4	51.3	50.9	50.8	0.079
3	56.8	57.2	56.7	58	57.9	57.7	57.4	0.079
4	71.8	72	71.5	73	72.7	72.5	72.3	0.000
5	74.8	74.9	74.5	75.1	74.9	74.7	74.8	0.006
6	75.6	75.9	75.4	76	75.9	75.6	75.7	0.031
7	76.1	76.3	75.9	76.5	76.3	76.2	76.2	0.033

Table B-2-6 Data of charging and discharging cycle of 2.0 wt% AC (Cont.)

Time (min)	Temperature (°C)						AVG	STD
	2.0 wt% AC (1)			2.0 wt% AC (2)				
	1st	2nd	3rd	1st	2nd	3rd		
8	76.3	76.4	75.9	76.7	76.4	76.3	76.3	0.040
9	76.4	76.5	76.3	76.7	76.4	76.3	76.4	0.076
10	76.5	76.6	76.4	76.7	76.4	76.4	76.5	0.052
11	76.6	76.7	76.5	76.8	76.4	76.5	76.6	0.076
12	76.7	76.7	76.5	76.8	76.5	76.6	76.6	0.026
13	76.7	76.7	76.6	76.8	76.5	76.6	76.7	0.067
14	76.7	76.8	76.6	76.8	76.5	76.7	76.7	0.037
15	76.8	76.8	76.7	76.8	76.5	76.7	76.7	0.067
16	76.8	76.8	76.7	76.9	76.6	76.7	76.8	0.067
17	76.9	76.8	76.7	76.9	76.6	76.7	76.8	0.037
18	76.9	76.9	76.8	76.9	76.6	76.7	76.8	0.067
19	76.9	76.9	76.8	76.9	76.7	76.7	76.8	0.041
20	76.9	76.9	76.8	76.9	76.7	76.8	76.8	0.030
21	57.2	56.8	57	57.7	57.5	57.3	57.3	0.000
22	44.0	43.7	43.9	44.7	44.4	44.5	44.2	0.000
23	40.9	40.6	40.7	41.1	40.9	41.0	40.9	0.037
24	39.9	39.5	39.7	40.5	40.0	40.2	40.0	0.037
25	38.5	38.2	38.3	39.3	38.9	39.2	38.7	0.039
26	37.6	37.3	37.4	37.9	37.7	37.8	37.6	0.037
27	36.0	35.7	35.9	36.3	36.0	36.1	36.0	0.000
28	34.9	34.5	35.0	35.4	35.0	35.1	35.0	0.040
29	33.9	33.3	33.6	34.2	33.8	34.0	33.8	0.071
30	32.4	32.1	32.3	32.8	32.5	32.7	32.5	0.000
31	31.7	31.3	31.6	32.0	31.6	31.9	31.7	0.000
32	31.1	30.6	30.9	31.6	31.3	31.5	31.2	0.070
33	30.9	30.5	30.6	31.1	30.8	30.9	30.8	0.039
34	30.8	30.5	30.5	31.0	30.7	30.8	30.7	0.014
35	30.7	30.4	30.5	31.0	30.6	30.8	30.7	0.033
36	30.6	30.4	30.4	30.9	30.6	30.7	30.6	0.026
37	30.6	30.4	30.4	30.8	30.5	30.6	30.6	0.026
38	30.5	30.3	30.4	30.7	30.5	30.6	30.5	0.000
39	30.5	30.3	30.4	30.7	30.5	30.6	30.5	0.000
40	30.5	30.3	30.2	30.6	30.5	30.5	30.4	0.067
41	30.4	30.3	30.2	30.6	30.4	30.5	30.4	0.000
42	30.4	30.3	30.2	30.6	30.4	30.5	30.4	0.000
43	30.4	30.2	30.2	30.6	30.4	30.5	30.4	0.011
44	30.3	30.2	30.2	30.5	30.4	30.4	30.3	0.000
45	30.3	30.2	30.2	30.5	30.4	30.4	30.3	0.000

Table B-2-6 Data of charging and discharging cycle of 2.0 wt% AC (Cont.)

Time (min)	Temperature (ºC)							
	2.0 wt% AC (1)			2.0 wt% AC (2)			AVG	STD
	1st	2nd	3rd	1st	2nd	3rd		
46	30.3	30.2	30.2	30.5	30.4	30.4	30.3	0.000
47	30.3	30.2	30.2	30.5	30.3	30.4	30.3	0.030
48	30.3	30.2	30.2	30.4	30.3	30.4	30.3	0.000
49	30.3	30.2	30.2	30.4	30.3	30.4	30.3	0.000
50	30.3	30.2	30.2	30.4	30.3	30.4	30.3	0.000

Table B-2-7 Data of charging and discharging cycle of 2.5 wt% AC

Time (min)	Temperature (ºC)							
	2.5 wt% AC (1)			2.5 wt% AC (2)			AVG	STD
	1st	2nd	3rd	1st	2nd	3rd		
0	31.9	31.9	31.9	31.9	31.9	31.9	31.9	0.000
1	47.2	47.1	46.9	48	47.6	47.9	47.5	0.039
2	54.5	54.2	53.9	55.1	55	54.9	54.6	0.141
3	61.0	60.8	60.6	61.8	61.6	61.6	61.2	0.060
4	75.4	75.2	75.1	76.3	75.9	76.0	75.7	0.039
5	76.5	76.4	76.3	77.2	77.1	77.1	76.8	0.030
6	76.5	76.6	76.5	77.3	77.1	77.2	76.9	0.030
7	76.9	76.6	76.5	77.3	77.2	77.3	77.0	0.106
8	76.9	76.6	76.5	77.3	77.2	77.3	77.0	0.106
9	77.3	77.0	77.0	77.3	77.2	77.3	77.2	0.082
10	77.3	77.1	77.0	77.3	77.2	77.3	77.2	0.067
11	77.4	77.1	77.0	77.3	77.2	77.3	77.2	0.106
12	77.4	77.1	77.0	77.3	77.3	77.3	77.2	0.147
13	77.4	77.1	77.1	77.3	77.3	77.3	77.3	0.122
14	77.4	77.1	77.1	77.3	77.3	77.3	77.3	0.122
15	77.5	77.2	77.1	77.3	77.3	77.4	77.3	0.106
16	77.5	77.2	77.1	77.4	77.3	77.4	77.3	0.106
17	77.5	77.2	77.2	77.4	77.3	77.4	77.3	0.082
18	77.5	77.2	77.2	77.4	77.3	77.4	77.3	0.082
19	77.5	77.3	77.3	77.4	77.3	77.4	77.4	0.041
20	77.5	77.3	77.3	77.4	77.4	77.4	77.4	0.082
21	56.7	56.2	56.4	56.7	56.9	60.0	57.2	1.130
22	42.5	41.9	42.2	42.4	42.6	42.8	42.4	0.071
23	39.7	39.3	39.5	39.9	40.0	40.3	39.8	0.006
24	38.4	38.0	38.3	38.3	38.6	38.8	38.4	0.031
25	37.4	36.9	37.1	37.4	37.6	37.9	37.4	0.000
26	36.3	35.8	36	36.5	36.5	37	36.4	0.026
27	34.8	34.5	34.6	34.7	35	35.4	34.8	0.140

Table B-2-7 Data of charging and discharging cycle of 2.5 wt% AC (Cont.)

Time (min)	Temperature (ºC)							
	2.5 wt% AC (1)			2.5 wt% AC (2)			AVG	STD
	1st	2nd	3rd	1st	2nd	3rd		
28	33.2	32.7	33.0	33.5	33.4	33.9	33.3	0.009
29	32.0	31.7	31.9	32.1	32.2	32.6	32.1	0.079
30	31.2	30.9	31	31.3	31.4	31.8	31.3	0.079
31	30.8	30.6	30.6	30.7	31.0	31.3	30.8	0.130
32	30.7	30.5	30.5	30.6	30.9	31.0	30.7	0.066
33	30.6	30.5	30.5	30.6	30.8	30.8	30.6	0.041
34	30.6	30.4	30.5	30.5	30.8	30.7	30.6	0.037
35	30.5	30.4	30.4	30.5	30.7	30.6	30.5	0.030
36	30.5	30.3	30.4	30.5	30.7	30.6	30.5	0.000
37	30.4	30.3	30.4	30.4	30.6	30.5	30.4	0.030
38	30.4	30.3	30.3	30.4	30.5	30.5	30.4	0.000
39	30.3	30.3	30.2	30.4	30.5	30.4	30.4	0.000
40	30.3	30.3	30.2	30.3	30.5	30.4	30.3	0.030
41	30.3	30.2	30.2	30.3	30.4	30.4	30.3	0.000
42	30.2	30.2	30.2	30.3	30.4	30.3	30.3	0.041
43	30.2	30.2	30.2	30.3	30.3	30.3	30.3	0.000
44	30.2	30.2	30.1	30.3	30.3	30.3	30.2	0.041
45	30.2	30.2	30.1	30.3	30.3	30.2	30.2	0.000
46	30.1	30.2	30.1	30.2	30.3	30.2	30.2	0.000
47	30.1	30.2	30.1	30.2	30.3	30.2	30.2	0.000
48	30.1	30.2	30.1	30.2	30.2	30.2	30.2	0.041
49	30.1	30.2	30.1	30.2	30.2	30.2	30.2	0.041
50	30.1	30.2	30.1	30.2	30.2	30.2	30.2	0.041

Table B-2-8 Result of latent heat from DSC analysis

Percentage by weight (%)	Latent heat (J/g)							
	Charging		Discharging		Total		AVG	STD
	1st	2nd	1st	2nd	1st	2nd		
pure palm wax	103.45	112.04	71.27	85.27	174.72	197.31	186.02	15.970
0.5 AC	97.23	107.19	71.63	84.90	168.86	192.09	180.47	16.430
1.0 AC	122.73	105.29	85.51	78.62	208.24	183.91	196.08	17.200
1.5 AC	113.74	97.98	76.92	74.39	190.66	172.37	181.51	12.930
2.0 AC	104.97	97.19	71.84	73.82	176.81	171.01	173.91	4.100
2.5 AC	107.79	95.66	71.98	70.24	179.77	165.90	172.83	9.810

Appendix B-3: Calculation of power of portable device

Example Determine heat transfer without PCM

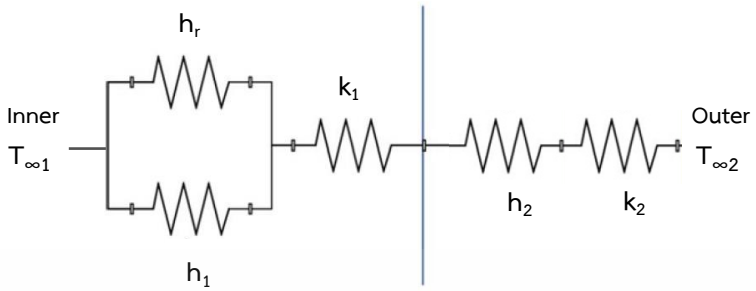

Figure 18 Heat transfer network of device without CPCM (side view)

Find $Q_{radiation}$ (h_r)

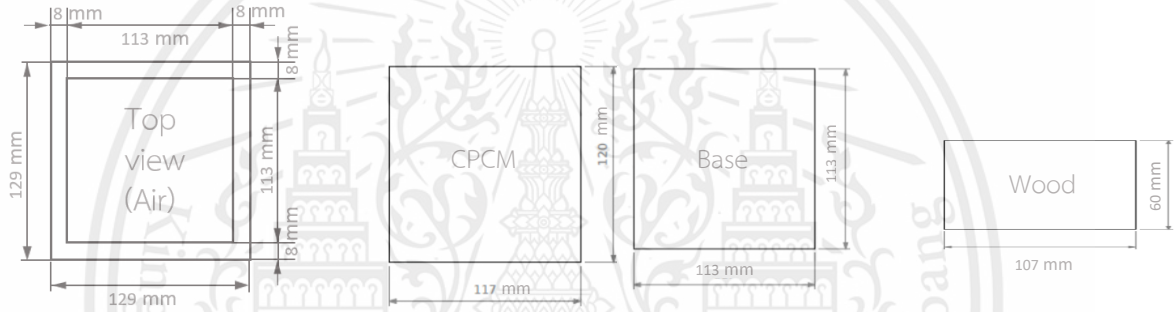

(a) (b) (C)

Figure 20 Area of device

(a) Area of air (b) Area of CPCM and base (c) Area of wood

Air → $A_1 = 113 \text{ mm} \times 113 \text{ mm} = 12769 \text{ mm}^2 = 0.0128 \text{ m}^2$

CPCM + base → $A_2 = 4 \times (117 \text{ mm} \times 120 \text{ mm}) + (113 \text{ mm} \times 113 \text{ mm}) = 68929 \text{ mm}^2$
$= 0.0689 \text{ m}^2$

Wood → $A_3 = 4 \times (107 \text{ mm} \times 60 \text{ mm}) = 25680 \text{ mm}^2 = 0.0257 \text{ m}^2$

Define : 1 is area of air

2 is area of CPCM and base

3 is area of wood

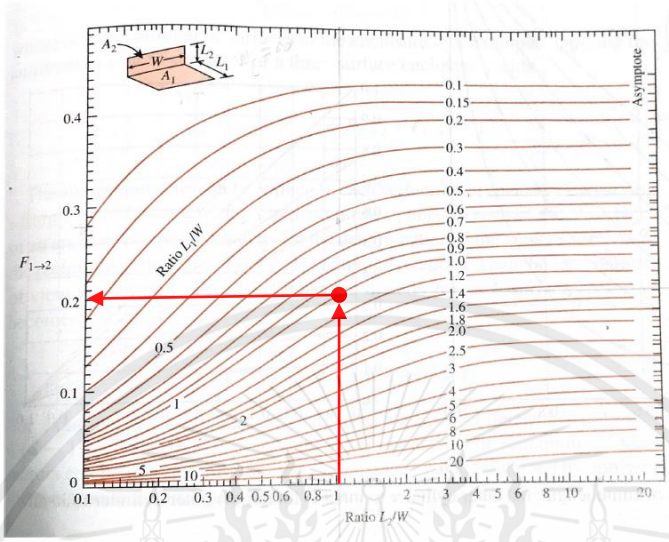

Ratio L_2/W = 120/117

= 1.02

Ratio L_1/W = 113/113

= 1

Figure 21 View factor between two perpendicular rectangles with a common edge

So, from Figure 21 : $F_{12} = 0.20$

From summation rule

$$\sum_{i=1}^{N} F_{i\to j} = 1$$

$$F_{11} + F_{12} + F_{13} = 1$$

$$F_{13} = 1 - F_{11} - F_{12}$$

$$F_{13} = 1 - 0 - 0.2$$

$$F_{13} = 0.80$$

$F_{11} = 0$

$F_{21} = F_{12} = 0.20$

$F_{23} = F_{32} = 0$

From $A_1 F_{13} = A_3 F_{31}$

$$F_{31} = F_{13} \times \frac{A_1}{A_3}$$

$$F_{31} = 0.80 \times \frac{0.0128}{0.0257}$$

$$F_{31} = 0.40$$

Constant :

- **Stefan-boltzmann constant (σ)** = 5.670 x 10^{-8} $W/m^2 K^4$
- **Emissivity of air (ε_1)** = 0.80
- **Emissivity of steel (ε_2)** = 0.36 - 0.44
- **Emissivity of wood (ε_3)** = 0.82 - 0.92

Air ; (i=1) $$\sigma T_1^4 = J_1 + \frac{1-\varepsilon_1}{\varepsilon_1}[F_{12}(J_1-J_2) + F_{13}(J_1-J_3)]$$

$$(5.67x10^{-8}\ W/m^2 K^4)(35+273\ K)^4 = J_1 + \left(\frac{1-0.8}{0.8}\right)[0.20(J_1-J_2) + 0.80(J_1-J_3)]$$

$$510.2530 = 1.25\,J_1 - 0.05\,J_2 - 0.20\,J_3 \quad \text{.....(1)}$$

PCM + base ; (i=2) $$\sigma T_2^4 = J_2 + \frac{1-\varepsilon_2}{\varepsilon_2}[F_{21}(J_2-J_1) + F_{23}(J_2-J_3)]$$

$$(5.67x10^{-8}\ W/m^2 K^4)(185+273\ K)^4 = J_2 + \left(\frac{1-0.36}{0.36}\right)[0.20(J_2-J_1) + 0]$$

$$2494.8553 = 1.36\,J_2 - 0.36\,J_1 \quad \text{.....(2)}$$

Wood ; (i=3) $$\sigma T_3^4 = J_3 + \frac{1-\varepsilon_3}{\varepsilon_3}[F_{31}(J_3-J_1) + F_{32}(J_3-J_2)]$$

$$(5.67x10^{-8}\ W/m^2 K^4)(700+273\ K)^4 = J_3 + \left(\frac{1-0.82}{0.82}\right)[0.40(J_3-J_1) + 0]$$

$$50819.9718 = 1.09J_3 - 0.09\,J_1 \quad \text{.....(3)}$$

Therfore,

J_1 = 8135.00 W/m^2

J_2 = 3987.83 W/m^2

J_3 = 47295.52 W/m^2

Find Q_{total}

$Q_1 = A_1[F_{1\to2}(J_1 - J_2) + F_{1\to3}(J_1 - J_3)]$

$= 0.0128 \times ((0.20 \text{ x } (8135.00 - 3987.83)) + (0.80 \text{ x } (8135.00 - 47295.52)))$

$Q_1 = -390.3870$ W

$Q_2 = A_2 [F_{2\to1} (J_2 - J_1) + F_{2\to3} (J_2 - J_3)]$

$= 0.0689 \times ((0.20 \times (3987.83 - 8135.00)) + 0)$

$Q_2 = -57.1480 \text{ W}$

$Q_3 = A_3 [F_{3\to1} (J_3 - J_1) + F_{3\to2} (J_3 - J_2)]$

$= 0.0257 \times ((0.40 \times (47295.52 - 8135.00)) + 0)$

$Q_2 = 402.5701 \text{ W}$

Then, $Q_{total} = Q_1 + Q_2 + Q_3$

$= -390.3870 \text{ W} - 57.1480 \text{ W} + 402.5701 \text{ W}$

$\therefore Q_{total} = -44.9649 \rightarrow \mathbf{Q_{radiation}\ (h_r)}$

Find $Q_{convection}(h_1)$

Film temperature (T_f) : $T_f = \frac{T_s - T_\infty}{2} = \frac{700 - 350}{2} = 175\ ^\circ\text{C}$

From table A-15: Properties of air at 1 atm pressure in textbook (Heat and Mass Transfer Fundamentals and Applications 5th Edition by Yunus A. Cengel and Afshin J. Ghajar);

$k = 0.03612 \text{ W/m•K}$

$\nu = 3.153 \times 10^{-5} \text{ m}^2/\text{s}$

$Pr = 0.6998$

$\beta = \frac{1}{T_f} = \frac{1}{175\ ^\circ\text{C} + 273 \text{ K}} = 2.2321 \times 10^{-3} \text{ 1/K}$

Rayleigh number (Ra_L) :

$$Ra_L = \frac{g\beta (T_1 - T_2) L_c^3}{\nu^2} Pr$$

$$Ra_L = \frac{(9.81 \text{ m/s}^2)(2.2321 \times 10^{-3} \text{ 1/K})(700 - 350 \text{ K})(0.12 \text{ m})^3}{(3.153 \times 10^{-5} \text{m}^2/\text{s})^2} (0.6998)$$

$Ra_L = 9322243.314$

Nusselt number (Nu) :

$$Nu = 0.42\ Ra_L^{1/4}\ Pr^{0.012}\ (H/\ L_v)^{-0.3}$$

$$= 0.42\ (9322243.314)^{1/4}(0.6998)^{0.012}\ (0.12/0.003)^{-0.3}$$

$$Nu = 7.6410$$

Find $Q_{convection}$

$$Q_{convection} = k\ Nu\ A_s \frac{(T_1-T_2)}{L_C}$$

$$= (0.03612\ W/m\bullet K) \times (7.6410) \times (4 \times (0.117m \times 0.120m) + (0.113\ m \times 0.113\ m)) \times \frac{(700-350)}{0.12}$$

$Q_{convection} = 55.4864\ W \rightarrow \mathbf{Q}_{convection}\ (h_1)$

Find $Q_{convection}(h_2)$

Film temperature (T_f) : $T_f = \frac{T_s - T_\infty}{2} = \frac{300\ ^oC - 230\ ^oC}{2} = 35\ ^oC$

From table A-15: Properties of air at 1 atm pressure in textbook (Heat and Mass Transfer Fundamentals and Applications 5th Edition by Yunus A. Cengel and Afshin J. Ghajar);

$$k = 0.02625\ W/m\bullet K$$

$$\nu = 1.655 \times 10^{-5}\ m^2/s$$

$$Pr = 0.7268$$

$$\beta = \frac{1}{T_f} = \frac{1}{35\ ^oC + 273\ K} = 3.2468 \times 10^{-3}\ 1/K$$

Rayleigh number (Ra_L) :

$$Ra_L = \frac{g\beta\ (T_1-T_2)\ L_c^3}{\nu^2}\ Pr$$

$$Ra_L = \frac{(9.81\ m/s^2)(3.2468 \times 10^{-3}\ 1/K)(300-230\ K)(0.12\ m)^3}{(1.655 \times 10^{-5} m^2/s)^2}\ (0.7268)$$

$$Ra_L = 10223162.06$$

Nusselt number (Nu) :

$$Nu = 0.42\ Ra_L^{1/4}\ Pr^{0.012}\ (H/\ L_v)^{-0.3}$$

$$= 0.42\ (10223162.06)^{1/4}(0.7268)^{0.012}\ (0.12/0.008)^{-0.3}$$

$$Nu = 10.4992$$

Find $Q_{convection}$

$$Q_{convection} = k\ Nu\ A_s \frac{(T_1-T_2)}{L_C}$$

$$= (0.02625\ W/m{\bullet}K) \times (10.4992) \times (4 \times (0.117\ m \times 0.120\ m)) \times \frac{(300-230)}{0.12}$$

$Q_{convection} = 9.0288\ W \rightarrow \mathbf{Q}_{convection}\ (h_2)$

Find $Q_{conduction}(k_1)$

Constant:

- Thermal conductivity of CPCM = 0.238 W/m·K
- Thermal conductivity of ss304 = 14.400 W/m·K

Then, $k_1 = k_3$

Resistance of conduction : $$R = \frac{L}{k_1 A} = \frac{0.001\ m}{(14.4\ W/m{\cdot}K) \times (0.117\ m \times 0.120\ m \times 4)}$$

$$R = 1.2365 \times 10^{-3}\ ^oC/W$$

Find $Q_{conduction}$

$$Q_{conduction} = \frac{(T_1-T_2)}{R_{total}}$$

$$Q_{conduction} = \frac{350 - 300\ ^oC}{(1.2365 \times 10^{-3}\ ^oC/W)}$$

$Q_{conduction} = 40436.7165\ W \rightarrow \mathbf{Q}_{conduction}\ (k_1)$

Find $Q_{conduction}(k_2)$

Resistance of conduction : $$R = \frac{L}{k_3 A} = \frac{0.001\ m}{(14.4\ W/m{\cdot}K) \times (0.117\ m \times 0.120\ m \times 4)}$$

$$R = 1.2365 \times 10^{-3}\ ^oC/W$$

Find $Q_{conduction}$

$$Q_{conduction} = \frac{(T_1 - T_2)}{R_{total}}$$

$$Q_{conduction} = \frac{230\text{-}180\ ^oC}{(1.2365 \times 10^{-3}\ ^oC/W)}$$

$$Q_{conduction} = 40436.7165\ W \rightarrow \mathbf{Q}_{conduction}\ (k_3)$$

Then,

$Q_{total} = -44.9649\ W + 55.4864\ W + 9.0288\ W + 40436.7165\ W + 40436.7165\ W$

$Q_{total} = 80892\ W \cong 80.9\ kW$

The power of portable device without CPCM is 80.9 kW

Example Determine power of portable device with PCM

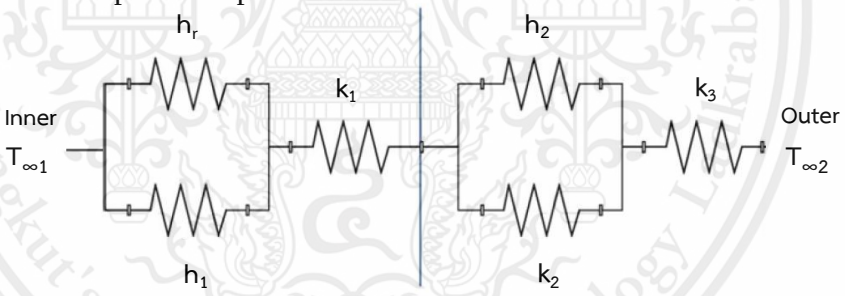

Figure 19 Heat transfer network of device with CPCM (side view)

Find $Q_{radiation}$ (h_r)

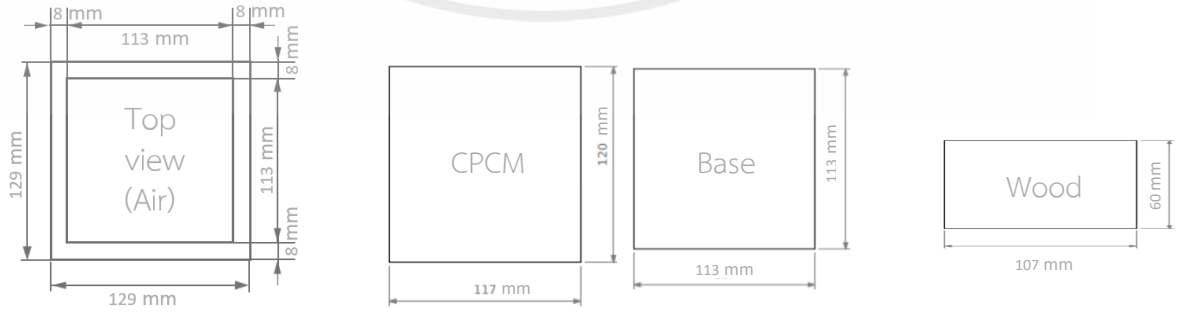

(a) (b) (C)

Figure 20 Area of device

(a) Area of air (b) Area of CPCM and base (c) Area of wood

Air → $A_1 = 113 \text{ mm} \times 113 \text{ mm} = 12769 \text{ mm}^2 = 0.0128 \text{ m}^2$

CPCM + base → $A_2 = 4 \times (117 \text{ mm} \times 120 \text{ mm}) + (113 \text{ mm} \times 113 \text{ mm}) = 68929 \text{ mm}^2$
$= 0.0689 \text{ m}^2$

Wood → $A_3 = 4 \times (107 \text{ mm} \times 60 \text{ mm}) = 25680 \text{ mm}^2 = 0.0257 \text{ m}^2$

Define : 1 is area of air

2 is area of CPCM and base

3 is area of wood

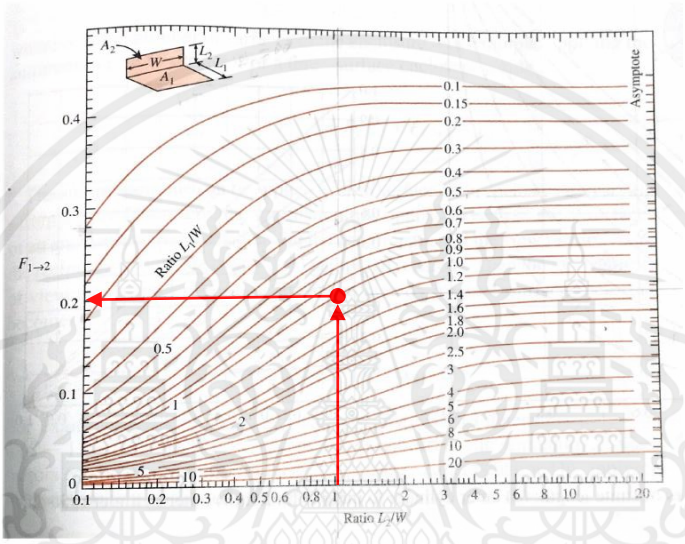

Ratio $L_2/W = 120/117$
$= 1.02$

Ratio $L_1/W = 113/113$
$= 1$

Figure 21 View factor between two perpendicular rectangles with a common edge

So, from Figure 21: $F_{12} = 0.20$

From summation rule

$$\sum_{i=1}^{N} F_{i\to j} = 1$$

$$F_{11} + F_{12} + F_{13} = 1$$

$$F_{13} = 1 - F_{11} - F_{12}$$

$$F_{13} = 1 - 0 - 0.2$$

$$F_{13} = 0.80$$

$F_{11} = 0$

$F_{21} = F_{12} = 0.20$

$F_{23} = F_{32} = 0$

From $A_1 F_{13} = A_3 F_{31}$

$$F_{31} = F_{13} \times \frac{A_1}{A_3}$$

$$F_{31} = 0.80 \times \frac{0.0128}{0.0257}$$

$$F_{31} = 0.40$$

Constant :

- **Stefan-boltzmann constant (σ)** = 5.670×10^{-8} W/m^2 K^4
- **Emissivity of air (ε_1)** = 0.80
- **Emissivity of steel (ε_2)** = 0.36 - 0.44
- **Emissivity of wood (ε_3)** = 0.82 - 0.92

Air ; (i=1) $\sigma T_1^4 = J_1 + \frac{1-\varepsilon_1}{\varepsilon_1}[\, F_{12}(J_1-J_2) + F_{13}(J_1-J_3)\,]$

$$(5.67\times10^{-8}\ \text{W/m}^2\text{K}^4)\,(35+273\ \text{K})^4 = J_1 + \left(\frac{1-0.8}{0.8}\right)[\, 0.20(J_1-J_2) + 0.80(J_1-J_3)\,]$$

$$510.2530 = 1.25\,J_1 - 0.05\,J_2 - 0.20\,J_3 \quad \text{.....(1)}$$

PCM + base ; (i=2) $\sigma T_2^4 = J_2 + \frac{1-\varepsilon_2}{\varepsilon_2}[\, F_{21}(J_2-J_1) + F_{23}(J_2-J_3)$

$$(5.67\times10^{-8}\ \text{W/m}^2\text{K}^4)\,(18\,5+273\ \text{K})^4 = J_2 + \left(\frac{1-0.36}{0.36}\right)[\, 0.20(J_2-J_1) + 0\,]$$

$$2494.8553 = 1.36\,J_2 - 0.36\,J_1 \quad \text{.....(2)}$$

Wood ; (i=3) $T_3^4 = J_3 + \frac{1-\varepsilon_3}{\varepsilon_3}[\, F_{31}(J_3-J_1) + F_{32}(J_3-J_2)\,]$

$$(5.67\times10^{-8}\ \text{W/m}^2\text{K}^4)\,(700+273\ \text{K})^4 = J_3 + \left(\frac{1-0.82}{0.82}\right)[\, 0.40(J_3-J_1) + 0\,]$$

$$50819.9718 = 1.09J_3 - 0.09\,J_1 \quad \text{.....(3)}$$

So,

$J_1 = 8135.00$ W/m^2

$J_2 = 3987.83$ W/m^2

$J_3 = 47295.52$ W/m^2

Find Q_{total}

$Q_1 = A_1 [F_{1\to2} (J_1 - J_2) + F_{1\to3} (J_1 - J_3)]$

$= 0.0128 \times ((0.20 \text{ x } (8135.00 - 3987.83)) + (0.80 \text{ x } (8135.00 - 47295.52)))$

$Q_1 = -390.3870 \text{ W}$

$Q_2 = A_2 [F_{2\to1} (J_2 - J_1) + F_{2\to3} (J_2 - J_3)]$

$= 0.0689 \times ((0.20 \times (3987.83 - 8135.00)) + 0)$

$Q_2 = -57.1480 \text{ W}$

$Q_3 = A_3 [F_{3\to1} (J_3 - J_1) + F_{3\to2} (J_3 - J_2)]$

$= 0.0257 \times ((0.40 \times (47295.52 - 8135.00)) + 0)$

$Q_2 = 402.5701 \text{ W}$

Then, $Q_{total} = Q_1 + Q_2 + Q_3$

$= -390.3870 \text{ W} - 57.1480 \text{ W} + 402.5701 \text{ W}$

$\therefore Q_{total} = -44.9649 \rightarrow \mathbf{Q_{radiation}\ (h_r)}$

Find $Q_{convection}(h_1)$

Film temperature (T_f) : $T_f = \frac{T_s - T_\infty}{2} = \frac{700 - 350}{2} = 175\ ^oC$

From table A-15: Properties of air at 1 atm pressure in textbook (Heat and Mass Transfer Fundamentals and Applications 5th Edition by Yunus A. Cengel and Afshin J. Ghajar);

$k = 0.03612 \text{ W/m•K}$

$\nu = 3.153 \text{ x } 10^{-5} \text{ m}^2/\text{s}$

$Pr = 0.6998$

$\beta = \frac{1}{T_f} = \frac{1}{175\ ^oC + 273 \text{ K}} = 2.2321 \text{ x } 10^{-3} \text{ 1/K}$

Rayleigh number (Ra_L) :

$$Ra_L = \frac{g\beta\ (T_1 - T_2)\ L_c^3}{\nu^2} Pr$$

$$Ra_L = \frac{(9.81 \text{ m/s}^2)(2.2321 \text{ x} 10^{-3} \text{ 1/K})(700\text{-}350 \text{ K})(0.12 \text{ m})^3}{(3.153 \text{ x} 10^{-5} \text{m}^2/\text{s})^2} (0.6998)$$

$Ra_L = 9322243.314$

Nusselt number (Nu) :

$$Nu = 0.42\ Ra_L^{1/4}\ Pr^{0.012}\ (H/\ L_v)^{-0.3}$$

$$= 0.42\ (9322243.314)^{1/4}(0.6998)^{0.012}\ (0.12/0.003)^{-0.3}$$

$$Nu = 7.6410$$

Find $Q_{convection}$

$$Q_{convection} = k\ Nu\ A_s \frac{(T_1-T_2)}{L_C}$$

$$= (0.03612\ W/m\bullet K) \times (7.6410) \times (4 \times (0.117\ m \times 0.120\ m) + (0.113\ m \times 0.113\ m)) \times \frac{(700-350)}{0.12}$$

$$Q_{convection} = 55.4864\ W \rightarrow \mathbf{Q}_{convection}\ (h_1)$$

Find $Q_{convection}(h_2)$

Film temperature (T_f) : $T_f = \frac{T_s - T_\infty}{2} = \frac{300 - 185}{2} = 57.5\ ^oC$

$k = 0.238\ W/m\bullet K$ (Obtained from TCA analysis)

$\nu = 4.1 \times 10^{-5}\ m^2/s$ (Obtained from paper [52])

$Pr = 10^2$ (Obtained from paper [53])

$$\beta = \frac{1}{T_f} = \frac{1}{57.5\ ^oC + 273\ K} = 3.0257 \times 10^{-3}\ 1/K$$

Rayleigh number (Ra_L) :

$$Ra_L = \frac{g\beta\ (T_1-T_2)\ L_c^3}{\nu^2} Pr$$

$$Ra_L = \frac{(9.81\ m/s^2)(3.0257 \times 10^{-3}\ 1/K)(300-185\ K)(0.12\ m)^3}{(4.1 \times 10^{-5} m^2/s)^2} (10^2)$$

$$Ra_L = 350807000.6$$

Nusselt number (Nu) :

• Pr of paraffin = 10^2

$$Nu = 0.42\ Ra_L^{1/4}\ Pr^{0.012}\ (H/\ L_v)^{-0.3}$$

$$= 0.42\ (350807000.6)^{1/4}(10^2)^{0.012}\ (0.12/0.008)^{-0.3}$$

$$Nu = 26.9580$$

Find $Q_{convection}$

$$Q_{convection} = k\ Nu\ A_s \frac{(T_1-T_2)}{L_C}$$

$$= (0.238\ W/m{\cdot}K) \times (26.9580) \times (4 \times (0.117\ m \times 0.120\ m)) \times \frac{(300-185)}{0.12}$$

$$Q_{convection} = 345.3093\ W$$

The latent heat of CPCM at 2.5 wt% AC, which is analyzed by using DSC is 165.90 J/g. The analysis of the CPCM sample at 2.5 wt% AC using DSC will use the sample weight of approximately 22.8000 mg. The started time of release electricity from device is around 8 minutes.

Then, the heat from CPM is

$$Q_{CPCM} = 165.90\ J/g \times 22.8000\ mg \times \frac{1}{8\ min} \times \frac{10^{-3}\ g}{1\ mg} \times \frac{1W}{1\ J/s} \times \frac{1\ min}{60\ s}$$

$$Q_{CPCM} = 7.8802 \times 10^{-3}\ W$$

So,

$$Q_{total} = \mathbf{Q}_{convection}(h_2) + Q_{CPCM}$$

$$= 345.3093\ W + 7.8802 \times 10^{-3}\ W$$

$$Q_{total} = 345.3172\ W \rightarrow \mathbf{Q}_{convection}(h_2)$$

Find $Q_{conduction}(k_1)$

Constant:

• Thermal conductivity of CPCM = 0.238 W/m·K

• Thermal conductivity of ss304 = 14.400 W/m·K

Then, $k_1 = k_3$

Resistance of conduction : $$R = \frac{L}{k_1 A} = \frac{0.001\ m}{(14.4\ W/m{\cdot}K) \times (0.117\ m \times 0.120\ m \times 4)}$$

$$R = 1.2365 \times 10^{-3}\ ^oC/W$$

Find $Q_{conduction}$

$$Q_{conduction} = \frac{(T_1 - T_2)}{R_{total}}$$

$$Q_{conduction} = \frac{350 - 300\ ^oC}{(1.2365 \times 10^{-3}\ ^oC/W)}$$

$$Q_{conduction} = 40436.7165\ W \rightarrow \mathbf{Q}_{conduction}\ (k_1)$$

Find $Q_{conduction}(k_2)$

Resistance of conduction : $$R = \frac{L}{k_2 A} = \frac{0.008\ m}{(0.238\ W/m{\cdot}K) \times (0.117\ m \times 0.120\ m \times 4)}$$

$$R = 0.59853\ ^oC/W$$

Find $Q_{conduction}$

$$Q_{conduction} = \frac{(T_1 - T_2)}{R_{total}}$$

$$Q_{conduction} = \frac{300 - 185\ ^oC}{0.59853\ ^oC/W}$$

$$Q_{conduction} = 192.1374\ W \rightarrow \mathbf{Q}_{conduction}\ (k_2)$$

Find $Q_{conduction}(k_3)$

Resistance of conduction : $$R = \frac{L}{k_3 A} = \frac{0.001\ m}{(14.4\ W/m{\cdot}K) \times (0.117\ m \times 0.120\ m \times 4)}$$

$$R = 1.2365 \times 10^{-3}\ ^oC/W$$

Find $Q_{conduction}$

$$Q_{conduction} = \frac{(T_1 - T_2)}{R_{total}}$$

$$Q_{conduction} = \frac{185 - 135\ ^oC}{(1.2365 \times 10^{-3}\ ^oC/W)}$$

$$Q_{conduction} = 40436.7164\ W \rightarrow \mathbf{Q}_{conduction}\ (k_3)$$

Then,

$\mathbf{Q_{total}}$ = -44.9649 W + 55.4864 W + 345.3172 W + 40436.7165 W + 192.1374 W + 40436.7165 W

$\mathbf{Q_{total}}$ = **81421.4091 W ≅ 81.4 kW**

The power of portable device without CPCM is 81.4 kW

Appendix B-4 Experimental result of experimental setup of prototype of a portable device

Table B-4-1 Data of Experimental setup of prototype of a portable device

No.	Times (min)			
	Start		End	
	without CPCM	with CPCM	without CPCM	with CPCM
1st	4.43	7.58	95.00	172.00
2nd	5.12	8.07	90.00	180.00
3rd	4.55	8.40	92.01	165.00
4th	5.41	8.00	90.00	173.00
5th	5.36	8.34	98.00	169.00
AVG	4.97	8.07	93.00	172.00
STD	0.457	0.326	3.464	5.540

BIBLIOGRAPHY

Name: Naruemon Nakmueng

Date of Birth: August 18, 1997

Address: 618 Wangthong Village, Soi Sawatdikan 2, Petchkasem 77 Road, Nong Khaem Sub-district, Nong Khaem District, Bangkok, Thailand 10160

E-mail: mind18081997@gmial.com, 59010708@kmitl.ac.th

Academic Background: Degree of Bachelor of Engineering
Department of chemical Engineering, Faculty of Engineering
King Mongkut's Institute of Technology Ladkrabang

Working Experience: Production Engineer at JSR BST Elastomer Co., LTD.

Name: Aroonroj Chaosukho

Date of Birth: March 17, 1998

Address: 90/182, krokyaicha street, Nernpra Sub-District,Mueng Rayong District, Rayong Province, Thailand 21150

E-mail: Aroonroj.ch17@gmail.com, 59011529@kmitl.ac.th

Academic Background: Degree of Bachelor of Engineering
Department of chemical Engineering, Faculty of Engineering
King Mongkut's Institute of Technology Ladkrabang

Working Experience: Production Engineer at JSR BST Elastomer Co., LTD.